

This article was downloaded by:

On: 21 January 2011

Access details: *Access Details: Free Access*

Publisher *Taylor & Francis*

Informa Ltd Registered in England and Wales Registered Number: 1072954 Registered office: Mortimer House, 37-41 Mortimer Street, London W1T 3JH, UK



## International Reviews in Physical Chemistry

Publication details, including instructions for authors and subscription information:

<http://www.informaworld.com/smpp/title~content=t713724383>

## Photoelectron Spectroscopy and Molecular Structure

W. C. Price<sup>a</sup>

<sup>a</sup> Wheatstone Physics Laboratory, King's College, Strand, London, UK

**To cite this Article** Price, W. C. (1981) 'Photoelectron Spectroscopy and Molecular Structure', *International Reviews in Physical Chemistry*, 1: 1, 1 – 30

**To link to this Article:** DOI: 10.1080/01442358109353240

**URL:** <http://dx.doi.org/10.1080/01442358109353240>

PLEASE SCROLL DOWN FOR ARTICLE

Full terms and conditions of use: <http://www.informaworld.com/terms-and-conditions-of-access.pdf>

This article may be used for research, teaching and private study purposes. Any substantial or systematic reproduction, re-distribution, re-selling, loan or sub-licensing, systematic supply or distribution in any form to anyone is expressly forbidden.

The publisher does not give any warranty express or implied or make any representation that the contents will be complete or accurate or up to date. The accuracy of any instructions, formulae and drug doses should be independently verified with primary sources. The publisher shall not be liable for any loss, actions, claims, proceedings, demand or costs or damages whatsoever or howsoever caused arising directly or indirectly in connection with or arising out of the use of this material.

## PHOTOELECTRON SPECTROSCOPY AND MOLECULAR STRUCTURE

W. C. PRICE

*Wheatstone Physics Laboratory, King's College, Strand, London WC2R 2LS, UK*

### ABSTRACT

A detailed description of how the electron cloud holds the various nuclei of a molecule together has for many years been the objective of the chemist, since this is fundamental to his subject and essential to its progress. The difficulties of acquiring this knowledge have now been largely overcome with the development of the technique of photoelectron spectroscopy. Using monoenergetic photon sources, such as the emission line of helium at 58.4 nm (21.22 eV), outer electrons can be ejected and their binding energies measured ( $E_B = h\nu - \frac{1}{2}mv^2$ ). Thus a quantitative description of the electronic environment of the nuclear framework is available for relating the electrical to the chemical properties of a molecule.

The present review deals with the ultraviolet photoelectron spectroscopy (UPS) of basic type molecules, illustrates the main features of the technique, and shows how the electronic structure determines the size and shape of the molecule. Much use is made of the isoelectronic principle to relate orbitals in different molecules and atoms. The use of X-ray photons to probe the core electrons is not discussed. Some emphasis is placed on the fact that the MO description, though very convenient for spectroscopy, is only one of the approximate ways of representing the statistical distribution of electrons in the negative charge cloud of a molecule.

### INTRODUCTION

Over the last decade the subject of photoelectron spectroscopy has developed at an enormous rate. It has acquired an immense literature and it has been necessary to establish a new journal to cope with the volume of research papers forthcoming from this and related fields. It is thus only possible in the present review to discuss the major features of photoelectron spectroscopy, to assess the impact it has had on our ideas of chemical bonding and to indicate some of the lines along which progress is being made. Like other forms of spectroscopy it investigates the electronic structures of molecular systems by studying their interaction with electromagnetic radiation. It is therefore appropriate to describe the energy states in terms of one-electron orbitals based on the symmetry of the system being studied since the magnitude of the transition moment which governs the radiative interaction is most directly related to these orbitals. This in no way invalidates the use of resonating bond structures based largely on interatomic distances used so successfully by Pauling from the 1930s. The data available then were about the nuclear framework. The data available from photoelectron spectroscopy concern mainly the electron cloud and its subdivision into electron orbitals. Most of the discussion which follows will be in terms of independent (distinguishable) electron orbitals, but it should always be remembered that even in atoms this is a simplification of the real situation.

Much of the early investigation of diatomic molecules was carried out by emission spectroscopy and by the late 1920s a fairly detailed understanding of their spectra and structure had been achieved. However, emission techniques were not successful in the study of polyatomic molecules because when subjected to electrical discharges large molecules become dissociated into diatomic fragments. The less disruptive techniques of absorption spectroscopy, however, brought some success and when the vacuum ultra-violet absorption spectra of many polyatomic molecules were investigated systems of bands were found which could be fitted into Rydberg series converging towards the first ionization potentials of these molecules. In this way accurate values were obtained for the binding energies of electrons in the  $\pi$  outer orbitals of acetylene, ethylene, and benzene. Sharp Rydberg series were also found for small molecules with non-bonding lone-pair  $p\pi$ -type electrons, as in  $\text{H}_2\text{O}$ ,  $\text{H}_2\text{S}$ ,  $\text{HCl}$ ,  $\text{HBr}$ ,  $\text{HI}$ ,  $\text{CO}_2$ ,  $\text{CS}_2$ ,  $\text{CH}_3\text{I}$  etc. (Price, 1936). These spectra were important since they provided confirmation of the molecular orbital approach to the theory of the electronic structure of polyatomic molecules which was being developed by Mulliken between 1930 and 1940. The absorption spectra of larger molecules were found to have broader and more diffuse bands than those of small molecules and, because of their overlapping, such bands could not be separated into series converging to ionization limits. Even in the case of small molecules, the bands which occurred at higher energies than the first ionization limit were also found to be so diffuse as to preclude their use for determining the binding energies of inner electrons.

Some progress in circumventing this impasse was made by Watanabe and his associates (Watanabe and Mottl, 1957) who measured the ion currents produced as the frequency of the photons incident upon a molecule was increased. They used a vacuum ultraviolet monochromator to scan photons of gradually increasing energies over the entrance slit to an ionization chamber containing the substance being studied. The wavelength at which photoionization set in was found to be relatively sharp, even when the ultraviolet absorption bands in the region of ionization were broad and diffuse. Thus the method yielded good first ionization potentials for molecules like methane, ethane and large polyatomic molecules such as, for example, substituted aromatics which did not have sufficiently well-defined band systems to show Rydberg series. The Watanabe method was not, however, capable of determining the ionization energies of inner orbitals any better than vacuum ultraviolet absorption spectroscopy, since it was found that as the photon energy was increased beyond the ionization threshold, large increases in ion current were obtained from processes associated with the autoionization of superexcited states, i.e. interactions between energetically equivalent states in which the excitation energy of an inner electron is transferred to ionize an electron from the outer orbital. These processes were of such a magnitude as to obscure any increases in ion current that might have arisen from the onset of ionization from the inner orbital. In order to avoid the effects of autoionization a further change of technique was required. This involved using a photon (line excitation) with an energy greater than that of any superexcited state of the electrons in the range being considered and measuring the energy of the ejected photoelectron, this energy being then subtracted from the energy of the incident photon in order to obtain the orbital binding energy. In this way it has been possible to observe and locate the inner orbitals of molecules without interference from electrons in outer orbitals. Although measurements of the energies of photoelectrons produced in photoionization studies of molecules were first carried out by Vilesov *et al.* in 1961, these workers were restricted in their studies to energies less than 11 eV because they employed a fluorite window to separate their photon source from their ion chamber. It was the use by Turner and his co-workers of the 21.22 eV resonance line of helium as a photon source and the avoidance of a window by utilizing differential pumping which formed the basis of the highly successful technique of ultraviolet photoelectron spectroscopy (UPS) as it is known today.

In a quite separate development during the late 1950s Kai Siegbahn and his coworkers at Uppsala were pioneering the use of X-ray sources to eject inner-core electrons. They used their experience in  $\beta$ -ray spectrometry to make the necessary technical development. Extensive details of the work of this school are given in two major publications (Siegbahn *et al.*, 1967 and 1969). More recently, monochromatized synchrotron radiation has been used to provide monoenergetic sources covering a wide wavelength range.

## EXPERIMENTAL

A schematic diagram of the equipment used in photoelectron spectroscopy is shown in Fig. 1. The monochromatic radiation, either UV or X-ray, impinges on the gas (or solid) under investigation in the sample chamber. The photoelectrons ejected by the radiation pass through the exit slit into an electrostatic electron energy analyser where after being separated by a radial (or cylindrical) electric field they pass through an exit slit and are detected by an electron multiplier. The energy spectrum of the photoelectrons emitted by the sample is obtained by plotting the count rate of the electrons arriving at the detector against the continuously increasing energy setting of the electron spectrometer. In the interaction the kinetic energy acquired by the heavy molecule is very much less than that of the photoelectron (in the ratio of the electron mass to the mass of the molecule). It can therefore be neglected as can also the effect of the thermal spread of molecular velocities. Thus the binding (or ionization) energy  $E$  of the photoelectron which is normally non-relativistic can be derived from the simple equation

$$E = h\nu - \frac{1}{2}mv^2. \quad (1)$$

It is customary in UPS to calibrate the scale of the electron spectrometer with reference gases of spectroscopically known ionization potentials rather than from the values of the voltages applied to the plates and the physical characteristics of the electron spectrometer. The former method is not usually possible in XPS and the kinetic energies of the

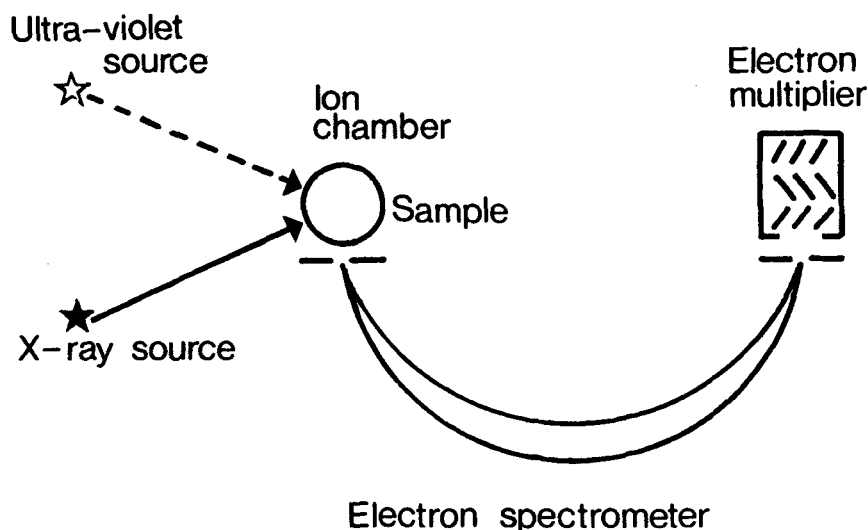


FIG. 1. Schematic diagram of ultraviolet/X-ray photoelectron spectrometer.

photoelectrons have to be measured by the direct method. Another significant difference between UPS and XPS is that whereas the line widths of the gaseous line sources in UPS are of the order of 0.002 eV those of XPS being derived from solid targets are seldom less than 0.2 eV even when monochromators are employed to limit the width of the line being used. Ultraviolet photoelectron spectrometry is therefore a more precise technique to use for studying electrons in valence and conduction bands whereas X-ray photoelectron spectroscopy is used largely to investigate core electrons which cannot be ejected by UV photons. The depths from which photoelectrons with the velocities encountered in practice can escape from solid samples are of the order of only a few angstroms. The technique is thus a surface one and is very valuable for this reason since gas/solid reactions depend upon the electrical conditions at the interfaces.

## ULTRAVIOLET PHOTOELECTRON SPECTROSCOPY

### *Monatomic gases*

For monatomic gases only electronic energy is involved in photoionization and the HeI photoelectron spectrum of atomic hydrogen consists of a single sharp peak corresponding to a group of photoelectrons with energies of 7.62 eV, i.e. equal to the difference in energy of the helium resonance line (21.22 eV) and the ionization of the H(1s) electron (13.60 eV). For argon the outer electrons are in p-type orbitals and the (3p)<sup>5</sup> configuration of the ion has the two states <sup>2</sup>P<sub>1/2</sub> and <sup>2</sup>P<sub>3/2</sub> with statistical weights in the ratio 2:1 and energies differing by spin-orbit coupling. The photoelectron spectrum (*see* Fig. 2) corresponding to this (3p)<sup>-1</sup> ionized state is thus a doublet, one component of which is twice as strong as the other. Similar doublets are found for the other inert gases, the spin-orbit coupling increasing with their atomic weight. Narrow line spectra corresponding to ionization of atoms to the lower states of their ions (i.e. ionization from each of the outer orbitals) have also been obtained for N, O, F, Cl, Br, I, Hg, Cd, and Zn.

Atomic systems relating as they do to a single positive nucleus involve the electron distribution in a central force field which is best described in terms of s, p, d orbitals. In molecules the simplest orbitals with which to describe the electron distribution are those appropriate to the symmetry of the nuclear framework. These are particularly suitable for discussing spectra because of the way they relate to the transition moment between states of different electronic energy. They are usually formulated by suitable linear combinations of atomic orbitals. For the photoejection of an electron from an orbital in a molecule we have the equation.

$$I_0 + E_{\text{vib}} + E_{\text{rot}} = h\nu - \frac{1}{2}mv^2 \quad (2)$$

where  $I_0$  is the 'adiabatic' ionization energy (i.e. the pure electronic energy change) and  $E_{\text{vib}}$  and  $E_{\text{rot}}$  are the changes in vibrational and rotational energy which accompany the photoionization. To explain the nature of the information which can be obtained, we shall discuss the photoelectron spectra of some simple molecules.

Figure 3(b) gives the potential curves of H<sub>2</sub> and H<sub>2</sub><sup>+</sup>. When an electron is removed from the neutral molecule the nuclei find themselves suddenly in the potential field appropriate to the H<sub>2</sub><sup>+</sup> ion but still separated by the distance characteristic of the neutral molecule. The most probable change is thus a transition on the potential energy diagram from the internuclear separation of the ground state to a point on the potential energy curve of the ion vertically above this. This is the Franck-Condon principle and it determines to which vibrational level of the ion the most probable transition (strongest band) occurs. The energy corresponding to this change is called the vertical ionization potential  $I_{\text{vert}}$ . Transitions to vibrational levels on either side of  $I_{\text{vert}}$  are weaker, the one of lowest energy

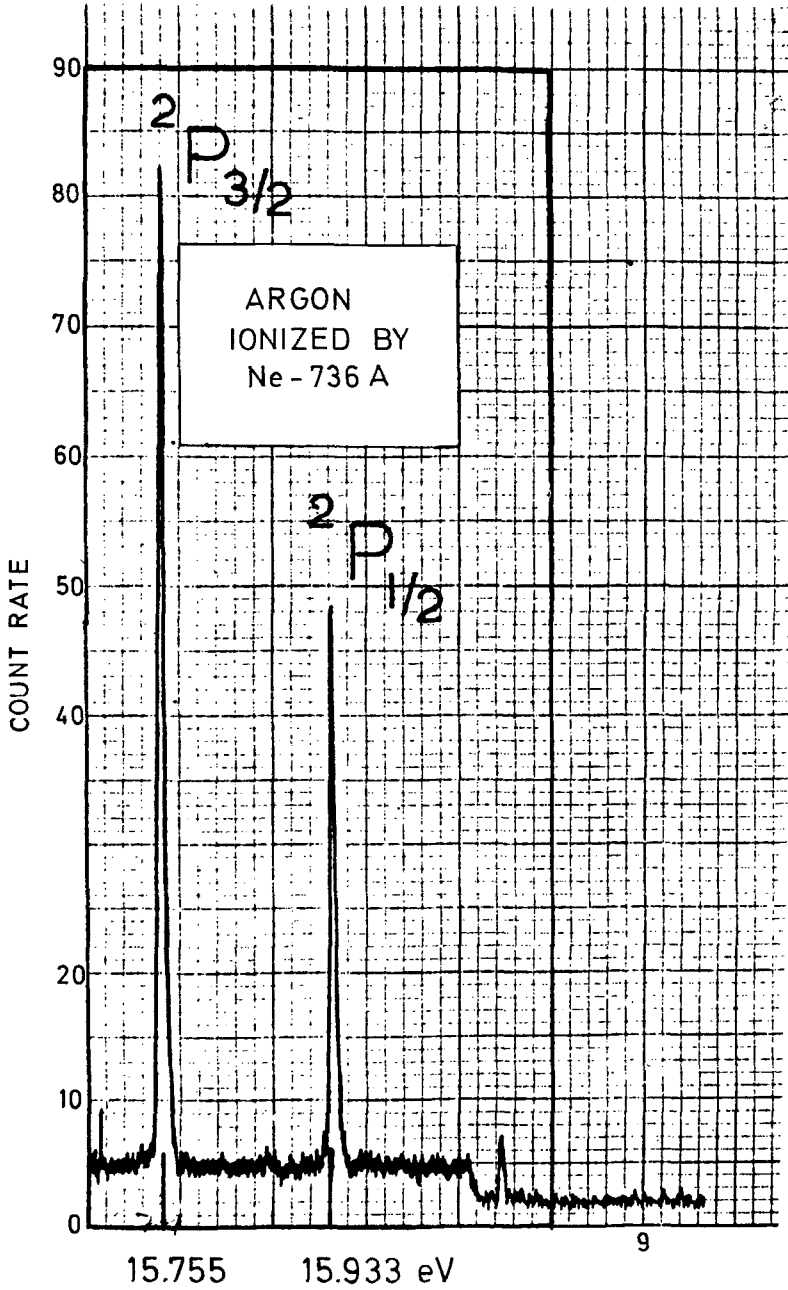


FIG. 2. Photoelectron spectrum of argon ionized by Ne I (73.6 nm).

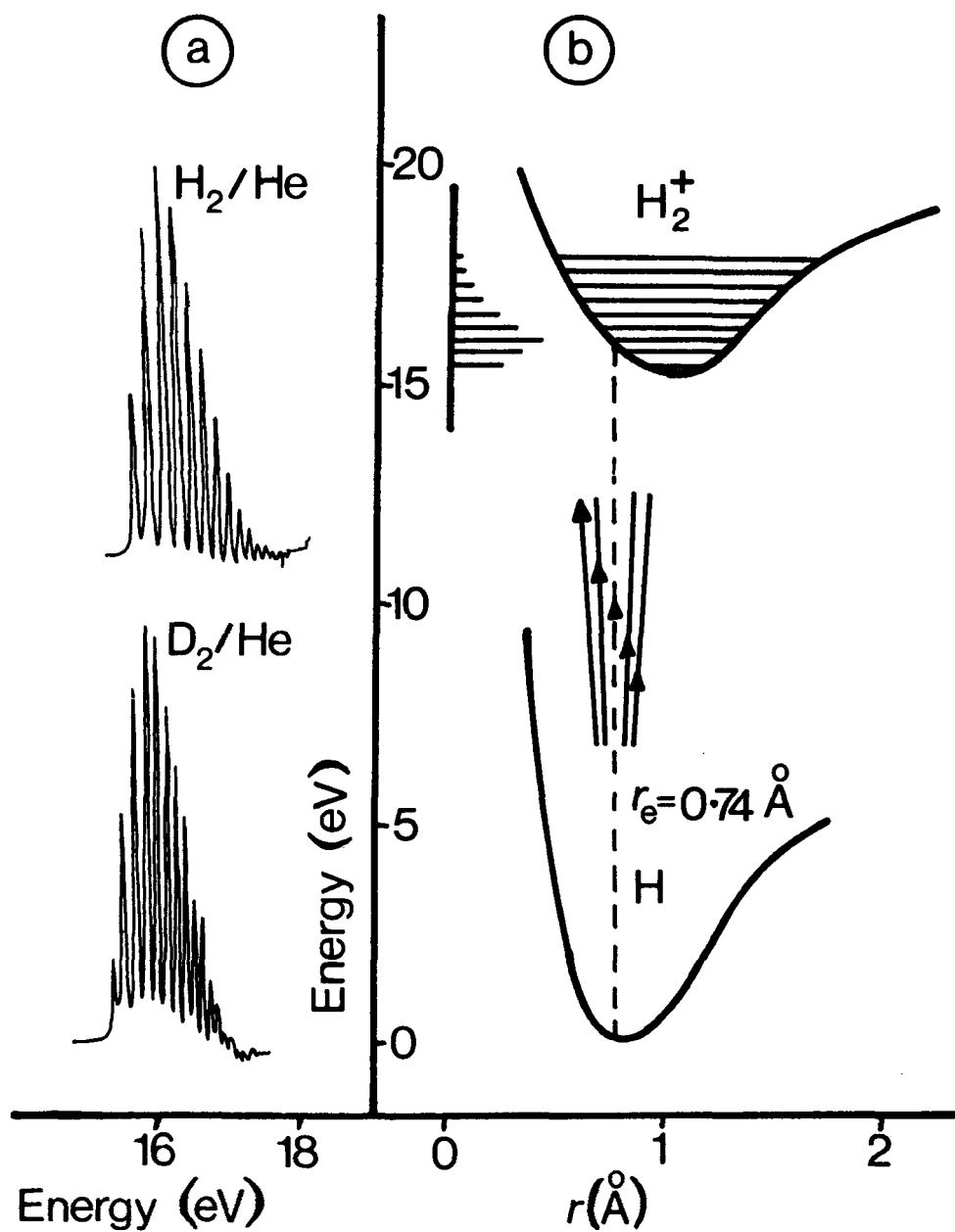


FIG. 3. (a) Photoelectron spectra of H<sub>2</sub> and D<sub>2</sub>; (b) potential energy curves of H<sub>2</sub> and H<sub>2</sub><sup>+</sup> showing spectra plotted along ordinate.

corresponding to the vibrationless state of the ion that is to  $I_{\text{adlab}}$ . The photoelectron spectra of  $\text{H}_2$  and  $\text{D}_2$  are given in Fig. 3(a) and that of  $\text{H}_2$  is also plotted along the ordinate of Fig. 3(b). It is worth noting that because one of the two bonding electrons is removed, the bonding energy at this internuclear distance should be approximately halved. Thus  $I_{\text{vert}}$  should be approximately equal to

$$I(\text{H}) + \frac{1}{2}D(\text{H}_2) = 13.595 + \frac{1}{2}(4.478) = 15.834 \text{ eV.} \quad (3)$$

This agrees as closely as  $I_{\text{vert}}$ , the maximum of the band envelope, can be estimated for  $\text{H}_2$ . However, in other molecules, e.g.  $\text{HCl}$ , the agreement is not so good due to compensating movements in other shells, i.e. deviations from Koopmans' Theorem (Koopmans, 1934) which assumes that the orbital binding energies of electrons are equal to the negative vertical ionization potentials.

It is possible to calculate the change in internuclear distance on ionization from the intensity distribution of the bands in the photoelectron spectrum. Clearly when a bonding electron is removed, the part of the photoelectron spectrum corresponding to this will show wide vibrational structure, with a frequency separation that is reduced from that of the ground-state vibration. The removal of relatively nonbonding electrons, on the other hand, will give rise to photoelectron spectra rather similar to those of the monatomic gases and little if any vibrational structure will accompany the main electronic band. The type of vibration associated with the pattern obtained when a bonding electron is removed can usually be identified as either a bending or a stretching mode and this can throw light on the function of the electron in the structure of the molecule, that is, either as angle-forming or distance-determining. From the band pattern it is frequently possible to calculate values of the changes in angle as well as changes in internuclear distance on ionization, and so the geometry of the ionic states can be found if that of the neutral molecule is known. Changes in bond lengths or angles can be calculated with about 10% accuracy for photoelectron band systems which show structure by using the semi-classical formula

$$(\Delta r)^2 = l^2(\Delta\theta)^2 = 0.543 (I_{\text{vert}} - I_{\text{adlab}}) \mu^{-1} \omega^{-2} \quad (4)$$

where  $r$  and  $l$  are in  $\text{\AA}$ ,  $\theta$  in radians,  $\mu$  in atomic units, and  $\omega$  the mean progression spacing in  $1000 \text{ cm}^{-1}$ .

#### *Photoelectron spectra of hydrides isoelectronic with the inert gases*

As examples of the features mentioned above and also to illustrate how the orbitals of isoelectronic systems are related to one another, we now discuss the photoelectron spectra of those simple hydrides for which the united atoms are the inert gases Ne, Ar, Kr, and Xe, that is, the atoms obtained by condensing all the nuclei into one central positive charge.

Hydrides such as  $\text{HF}$ ,  $\text{H}_2\text{O}$ ,  $\text{NH}_3$  and  $\text{CH}_4$  can be thought of as being formed from Ne by successively partitioning off protons from its nucleus. The solutions of the wave equation—the wave functions or orbitals—arising from the progressive subdivision of the positive charge pass continuously from the atomic to the molecular cases with a gradual splitting of the  $p^6$ -orbital degeneracy as the internal molecular fields are set up. It can be shown that the forces on the nuclei are just the classical electrostatic attractions which arise between them and the 'electron' charge distribution offset by the internuclear repulsions (Feynman, 1939). Schematic diagrams of the orbital changes are indicated in Fig. 4. The photoelectron spectra shown in Fig. 5(a)—(e) reveal this orbital subdivision in a striking way.

Figure 5(b) shows the spectra of the halogen acids which represent the first stage in this process. The spectra of the corresponding inert gas (i.e. the united atom) are given in Fig.



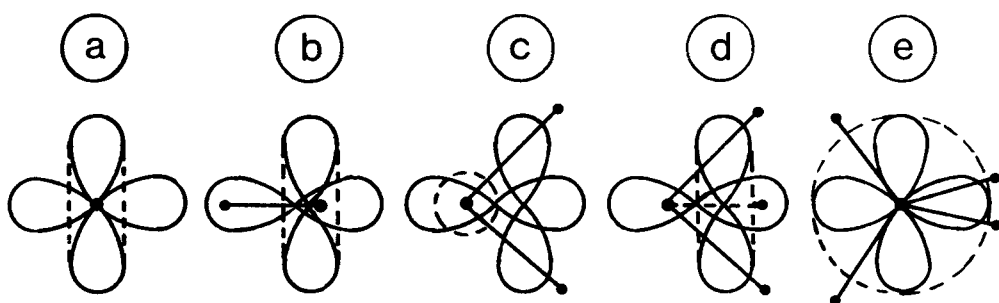


FIG. 4. Schematic diagrams of 2p-orbital structures of (a) Ne, (b) HF, (c) H<sub>2</sub>O, (d) NH<sub>3</sub> and (e) CH<sub>4</sub>.

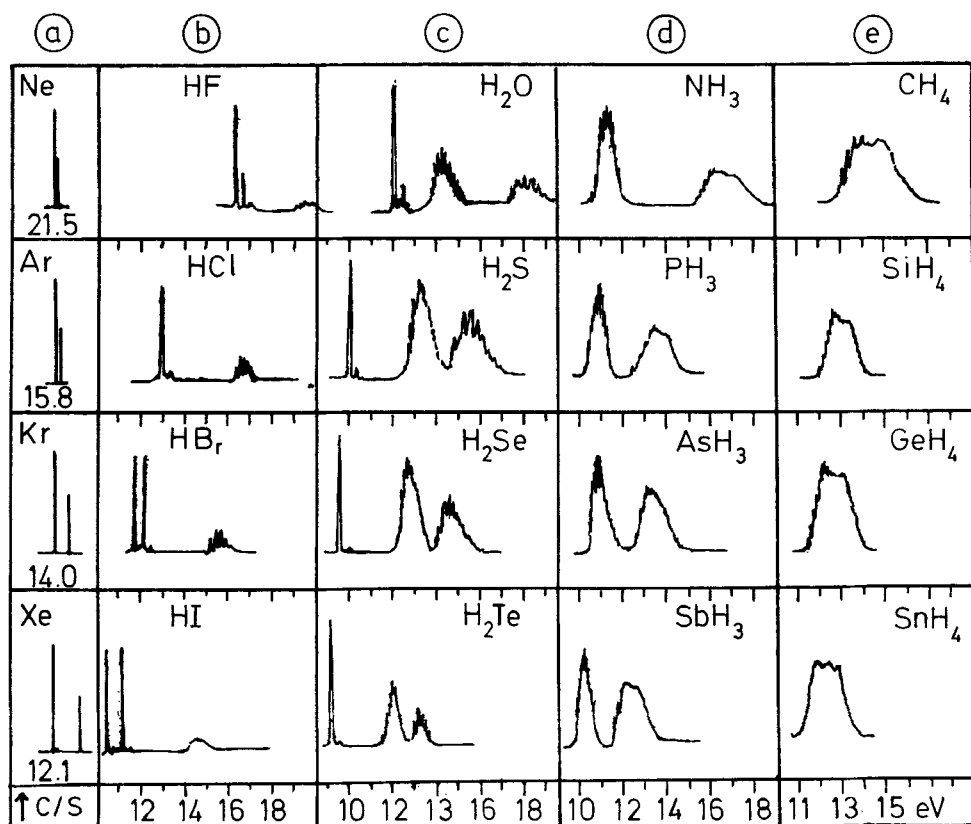


FIG. 5. Photoelectron spectra of the hydrides isoelectronic with Ne, Ar, Kr and Xe obtained with He (21.22 eV) radiation.

5(a). In going from the atom to the diatomic molecule, the triply degenerate  $p^6$  shell is split into a doubly degenerate  $\pi^4$  shell and a single degenerate  $\sigma^2$  shell. The  $\pi^4$  shell is non-bonding and represented by two bands in the photoelectron spectrum which are of equal intensity and show little vibrational structure. The  $\sigma$  shell is formed from the  $p$  orbital along

which the proton is extracted and gives a negative cloud which binds the proton to the residual positive charge. This  $p\sigma$  orbital therefore gives rise in the photoelectron spectrum to a simple progression of bands with a separation corresponding to the vibration frequency of the  ${}^2\Sigma^+$  state of the ion, except where the structure is lost by predissociation.

The second stage of partition leads to the molecules  $\text{H}_2\text{O}$ ,  $\text{H}_2\text{S}$ ,  $\text{H}_2\text{Se}$  and  $\text{H}_2\text{Te}$ . If two protons were removed *co-linearly* from the united atom nucleus, the linear triatomic molecule so formed would not have maximum stability, since only the two electrons in the  $p$  orbital lying along the line will then be effective in shielding the protons from the repulsion of the core. By moving off this line, the protons can acquire additional shelter from the central charge and from themselves through shielding by one lobe of a perpendicular  $p$  orbital (see Fig. 4(c)). The electrons in this orbital then become 'angle determining' as distinct from the two previously mentioned  $p$  electrons which are mainly effective in determining the bond separations of the hydrogen atoms from the central atom. The remaining  $p$  orbital, because of its perpendicular orientation to the plane of the bent  $\text{H}_2\text{X}$  molecule, can affect neither the bonding nor the angle, that is, its electrons are nonbonding. These expectations are borne out by the photoelectron spectra shown in Fig. 5(c). These spectra show how in all  $\text{H}_2\text{X}$  molecules, the triple degeneracy of the  $p^6$  shell of the united atom is completely split into three mutually perpendicular orbitals of different ionization energies. The lowest ionization band is sharp, with little vibrational structure. The second has a wide vibrational pattern which turns out to be the bending vibration of the molecular ion. The third also has a wide vibrational pattern with band separations greater than those of the second band. These separations can be identified as the symmetrical bond stretching vibrations of the ion. The geometries of these three ionized states can be calculated from the band envelopes and pattern spacings. Only small changes are associated with the band of lowest ionization potential. Large changes of angle accompany ionization in the second band, which in the case of  $\text{H}_2\text{O}$  causes the equilibrium configuration of this ionized state to be linear. In  $\text{H}_2\text{S}$ ,  $\text{H}_2\text{Se}$  and  $\text{H}_2\text{Te}$  the spectra show that the angles in the ion are  $129^\circ$ ,  $126^\circ$  and  $124^\circ$ , respectively. The third ionized state is one in which the internuclear distances are increased but little change occurs in the bond angle. The integrated intensities of all three bands are roughly equal, indicating that each originates from the ionization of a single orbital.

The partitioning of three protons from the nucleus of an inert gas molecule leads to a pyramidal  $\text{XH}_3$  molecule. One  $p$  orbital is directed along the axis of symmetry and provides the shielding which causes the molecule to have a nonplanar geometry, that is, it is angle-determining. The other two  $p$  orbitals are degenerate and provide an annular cloud of negative charge passing through the three  $\text{XH}$  bonds and thus mainly determine the bond distances. The structure pattern on the first band of the photoelectron spectrum (Fig. 5(d)) can be assigned to bending vibrations and indicates that the molecule flies to a symmetrical planar configuration without much change in the bond distances when an electron is ionized from this orbital. The second band in the photoelectron spectrum shows Jahn-Teller splitting which is consistent with its being doubly degenerate. Although it has limited structure, such structure as can be observed corresponds to changes in bond stretching without much change in bond angle.

Finally the photoelectron spectra of the  $\text{XH}_4$ -type molecules show that the  $p^6$  shell of the united atom has changed to another triply degenerate shell with orbitals of tetrahedral symmetry. The contour shows the presence of Jahn-Teller splitting, and the structure on the low-energy side shows that on ionization the molecule moves by contraction along one side of the enveloping cube towards a square coplanar configuration. The structure on the high-energy side indicates movement in the opposite direction toward two mutually perpendicular configurations in which opposite  $\text{XH}_2$  angles are roughly  $90^\circ$ . In the heavier molecules, for example  $\text{SnH}_4$ , the large spin-orbit splitting of the heavy atom influences the

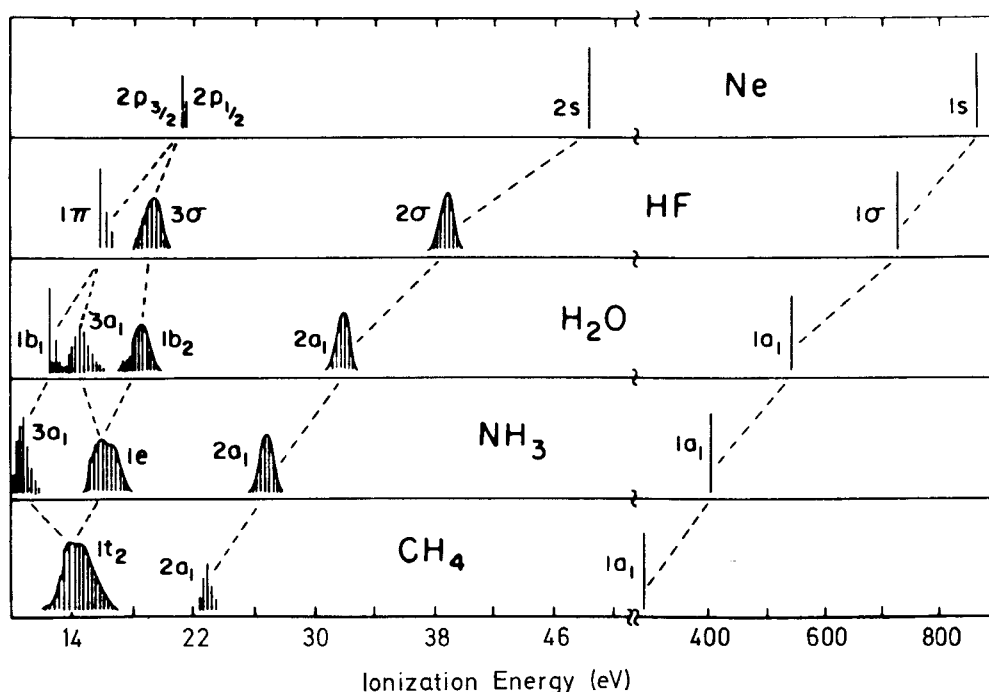


FIG. 6. Diagrammatic photoelectron spectra of the hydrides isoelectronic with neon indicating the splitting of the atomic into the molecular orbitals as the positive charge is subdivided.

structure. The spectra also show that the movement toward coplanarity is progressively less pronounced. Further details on the spectra of these hydride molecules are given by Potts and Price (1972).

It should be mentioned that the process of partitioning off protons from the neon nucleus to form the second two hydrides involves distortion of the 2s orbitals, though to a lesser extent than the 2p orbitals. They are deformed from spherical symmetry in the direction of the extracted proton. They thus have 'bumps' in the bond directions and in this way provide an 's' contribution to the bond. This is evident in the vibrational structure of the photoelectron bands associated with ionization from these orbitals. Figure 6 shows how the orbitals of the hydrides of F, N, O and C are formed by proton withdrawal from neon.

#### *Photoelectron spectra of the halogen derivatives of methane*

It is convenient to discuss at this point the photoelectron spectra of some 'single-bond' molecules in which some of the atoms have additional groups of nonbonding electrons. The bromomethanes, whose photoelectron spectra are illustrated in Fig. 7, are good examples of this molecular type. It can be seen that some bands in their spectra are relatively sharp and therefore can be associated with the nonbonding electrons, while others are broad and clearly arise from electrons in strongly bonding orbitals. The orbital assignments of the latter bands are indicated schematically in the figure. A comparison of these bands with those of the hydrides of the same symmetry, e.g.  $\text{CH}_3\text{Br}$  with  $\text{NH}_3$ ,  $\text{CH}_2\text{Br}_2$  with  $\text{H}_2\text{O}$ , etc., shows that the orbitals around the carbon atom are split up in very much the same way as

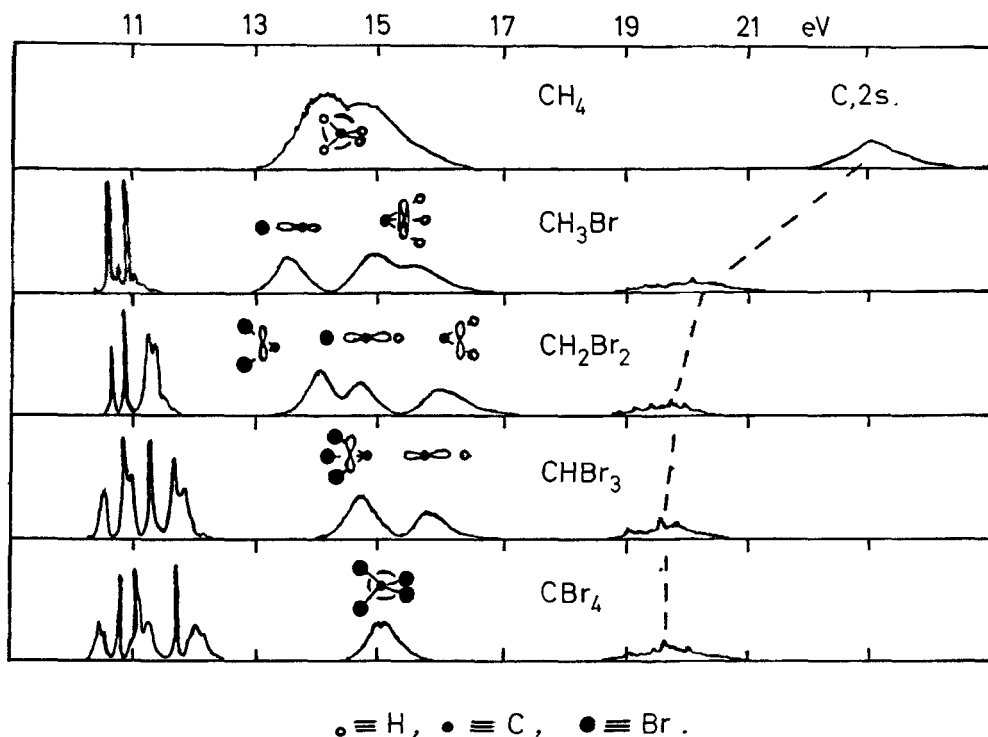


FIG. 7. Photoelectron spectra of the bromomethanes.

in the hydrides by the departure from tetrahedral symmetry brought about by the halogen substitution. This gives some support to the old concept that around an atom in a stable molecule there should be a closed (inert-gas) shell of electrons. It shows further how the degeneracy of the  $p^6$  group of these electrons is split by the fields arising from the different substituents, the splitting of the degeneracy being complete in the case of the methylene halide, as it is for water in the hydrides. The sharp bands in the region of 11 eV can be readily associated with orbitals containing 4p Br electrons which are split by spin-orbit interaction. In the case of methyl bromide two sharp bands (with very weak accompanying vibrational structure) are split by the magnitude of the spin-orbit coupling constant which is 0.32 eV for bromine. Further splitting occurs as the number of bromine atoms increases and eight bands can be seen in  $\text{CBr}_4$  corresponding to the eight nonbonding 'p' orbitals present in this molecule. A detailed account of the analysis of the photoelectron spectra of the halides of elements in groups III, IV, V and VI of the periodic table has been given by Potts *et al.* (1969, 1970).

#### *Photoelectron spectra of 'multiple' bonded diatomic molecules*

To discuss 'multiple' bonded systems in which molecular orbitals are formed by p atomic orbitals combining in the 'broadside-on' as well as in the 'end-on' configuration, we shall take as examples the molecules  $\text{N}_2$ , NO,  $\text{O}_2$  and  $\text{F}_2$ . Their photoelectron spectra are shown in Fig. 8. The orbitals upon which their electronic structures are built are the in-phase and out-of-phase combinations of the appropriate 2s and 2p orbitals. These are given schematically in the insert. For  $\text{N}_2$  the electronic configuration is  $(\sigma_g 2s)^2 (\sigma_u 2s)^2 (\pi_u 2p)^4$ .

$(\sigma_g 2p)^2$ , the orbitals being in order of decreasing ionization energy. With the exception of  $(\sigma_u 2s)$ , all of these might be expected to provide excess negative charge density between the two nuclei and thus to account for the strength of the  $N_2$  'triple' bond. The additional electron of NO has to go into a  $\pi^* 2p$  orbital which is largely outside the nuclei and therefore antibonding, and so, in a loose analogy,  $N_2$  is the 'inert gas' of diatomic molecules and NO the corresponding 'alkali metal', since it contains one electron outside a closed shell of bonding electrons. An inspection of the photoelectron spectrum of  $N_2$ , in which the ionized states corresponding to removal of the different orbital electrons are marked, shows that by far the most vibration accompanies the removal of the  $\pi_u$  electron. Thus at the internuclear distance of neutral  $N_2$ , the nuclei are held mainly by the negative cloud of the  $(\pi_u 2p)^4$  electrons. The short-distance bonding character of these  $\pi$  electrons results in the nuclei being pulled through the  $(\sigma 2p)^2$  cloud so that this  $\sigma$  orbital is as much outside the nuclei as between them and therefore supplies no bonding at the N–N equilibrium separation. It can be understood readily from the geometry of their overlap that the bonding of p electrons in the broadside-on ( $\pi$ ) arrangement optimizes at shorter internuclear distances than that in the end-on ( $\sigma$ ) position. In  $N_2$  the nuclei are in fact on the inside of the minimum of the partial potential energy curve associated with the  $(\sigma_g 2p)^2$  electrons. This orbital can thus be considered to be in compression, and its electrons have both their bonding and their binding (ionization) energies reduced. In NO,  $O_2$  and  $F_2$  the presence of the additional electrons in antibonding  $\pi 2p$  orbitals causes the internuclear distances to be relatively longer than they are in  $N_2$ , and it can be seen from Fig. 8 that the  $\sigma_g 2p$  bands of these molecules have progressively more vibrational structure as the internuclear distance approaches more closely that separation for which the bonding of the  $(\sigma_g 2p)^2$  orbital is optimized. The associated  $\sigma$  bands move through the  $\pi 2p$  systems to higher ionization energies in accord with their increased effective bonding power. For a fuller discussion, see Price (1977).

Other interesting points illustrated by Fig. 8 are that the spacing in the 2p antibonding bands in NO and  $O_2$  (first systems) are larger than those of the 2p bonding bands (second systems). This is to be expected since the removal of an antibonding electron increases the vibration frequency, while that of a bonding electron decreases this frequency. Another interesting feature is that the separation of the first and second bands, which reflects the overlap between the out-of-phase and in-phase ( $\pi 2p$ ) orbital, rapidly decreases with increase in internuclear distance. For NO,  $O_2$  and  $F_2$  these separations are 7.5, 4.5 and 3.0 eV, respectively. This indicates the reduction in 'multiple' ( $\pi$ ) bonding as the effect of the increasing number of  $\pi$  antibonding electrons reduces and annuls the bonding of  $\pi$  bonding electrons by increasing the interatomic distance and reducing the orbital overlap.

The insert of the 16–18 eV region of NO in Fig. 8 shows the  $^3\Pi$  and  $^1\Pi$  bands with an intensity ratio of 3:1, and thus illustrates how closely the intensities follow the statistical weights of the ionized states, agreeing with the number of channels of escape open to the electrons. Similar remarks apply to the  $^4\Sigma$  and  $^2\Sigma$  bands of  $O_2$ , the integrated intensities of which are in the ratio of 2:1. A further interesting feature which these multiplets illustrate is the greater bonding of the states of lower multiplicity. Since the lower multiplicity corresponds to the states of antisymmetric spin function, it is associated with the symmetric (summed) space coordinate wavefunction of the orbitals between which the spin interaction is occurring. The additional overlap to which this gives rise results in greater bonding relative to states of higher multiplicity, where the total space coordinate wavefunction is obtained by subtracting those of the interacting states.

The photoelectron spectrum contains enough information to plot a rough potential energy diagram of the states of the molecular ion provided the internuclear distance of the neutral species is known. The shape of the curve is obtained from the vibrational spacing. By placing the energy point corresponding to the maximum of the vibrational pattern at the

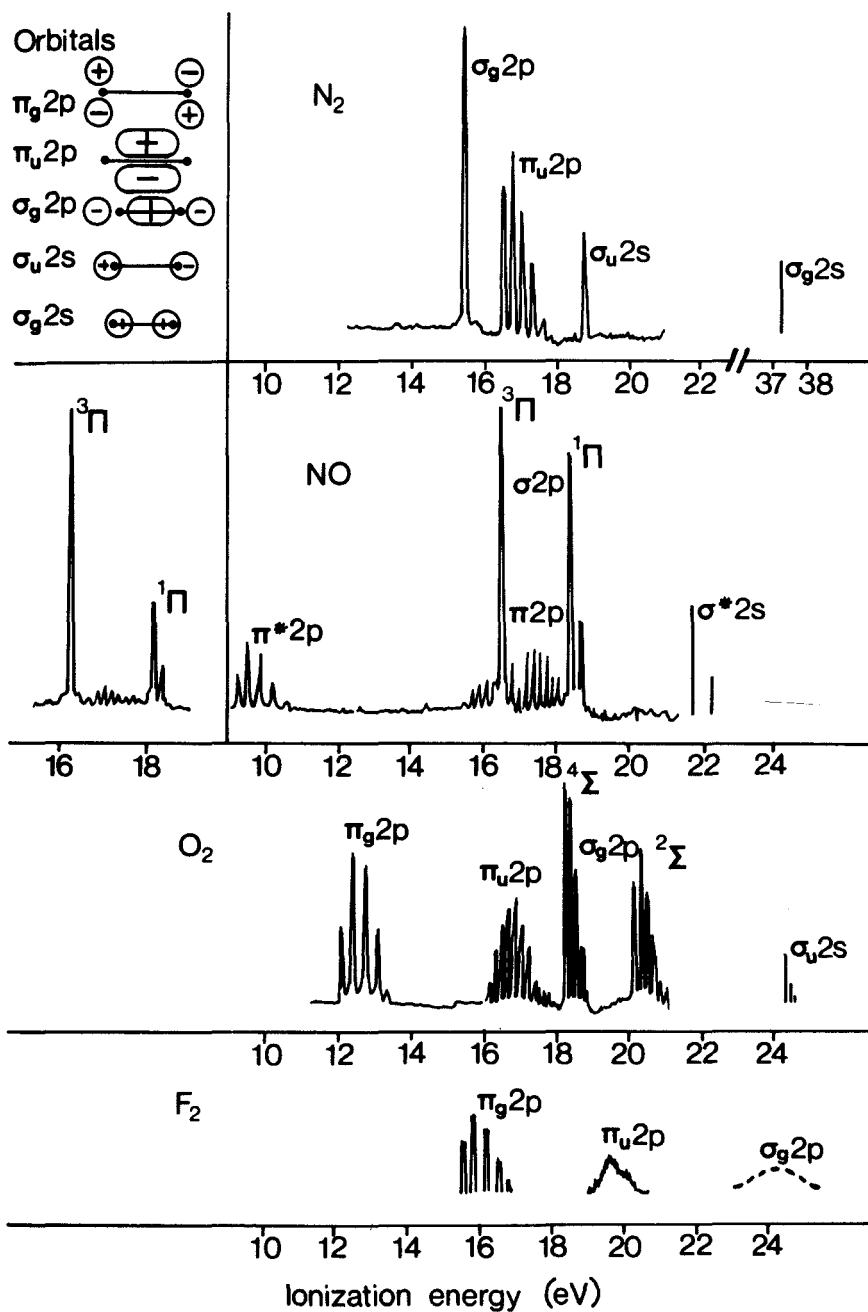


FIG. 8. Photoelectron spectra of N<sub>2</sub>, NO, O<sub>2</sub> and F<sub>2</sub>.

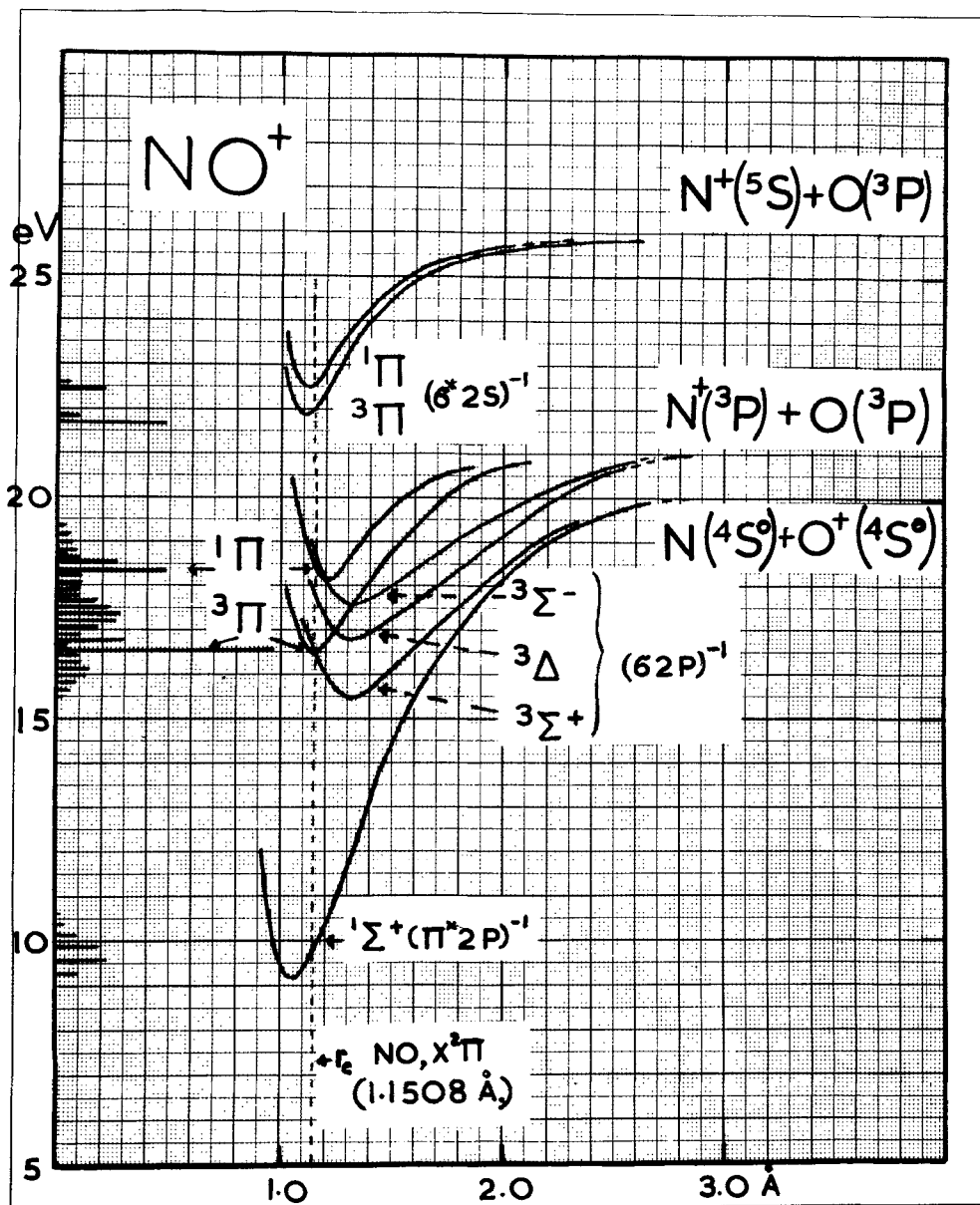


FIG. 9. Potential energy curves of  $\text{NO}^+$  showing relation to the photoelectron spectrum plotted along OY.

internuclear distance of the neutral molecule, its position on the horizontal scale can be fixed. That on the vertical scale is fixed by the ionization energy found for the  $v' = 0$  band. Internuclear separations for excited states can then be read off the diagram. This is illustrated for  $\text{NO}^+$  in Fig. 9, where the photoelectron spectrum is plotted along the OY axis of the potential-energy diagram.

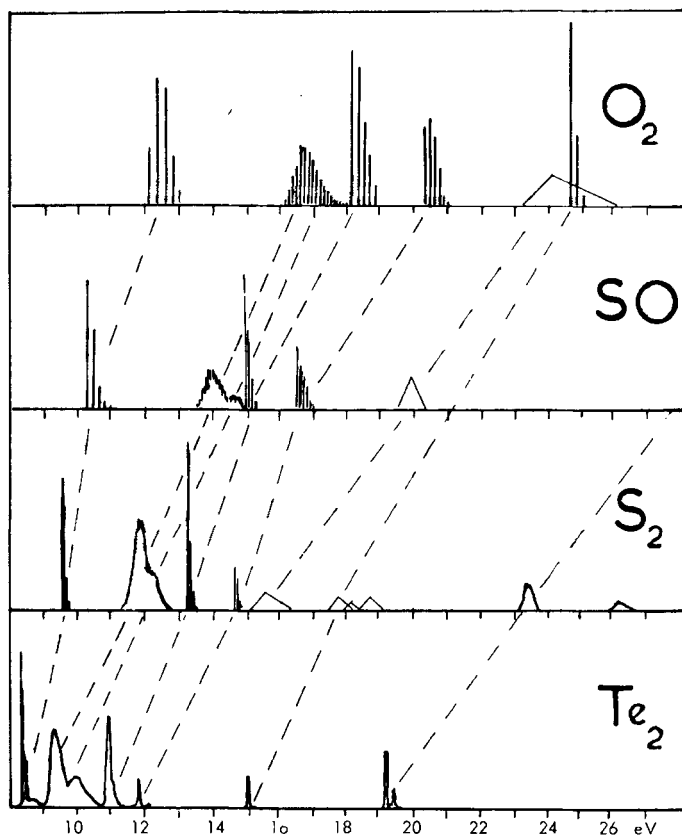


FIG. 10. Photoelectron spectra of the isoelectronic molecules  $O_2$ ,  $SO$ ,  $S_2$  and  $Te_2$ .

The variation of orbital energies of isoelectronic molecules with increasing mass of the constituent atoms is illustrated by the spectra of  $O_2$ ,  $SO$ ,  $S_2$  and  $Te_2$  shown in Fig. 10. The smaller orbital overlap arising from the greater spread of the orbitals of the heavier atoms reduces both their respective bonding and antibonding characters. This is evident from the reduced widths of the corresponding bands.

The 'building up' of the electronic structures of molecules by adding electrons to the unfilled orbitals as an atom is changed to one with greater  $Z$  follows very closely the 'aufbau' process in atoms. Although we have considered this only for diatomic molecules, it can be applied to triatomic and polyatomic systems and extends the shell concept to even the valence electrons of molecules. The difference between atoms and molecules is simply that instead of the positive charge being concentrated at one point, it is split into several different centres. It might be asked whether we should now replace the bond structures of chemists by the molecular orbital description. No spectroscopist, for example, has ever seen an electron in a hybridized  $sp^3$  orbital—a concept the chemist uses constantly. No real conflict exists, since the bond between the atoms is measured by the amount of negative charge lying between the two positive centres. From the orbital point of view this is made up by contributions from two orbitals, for example, in  $CH_4$  from the  $(2p_t)_6$  orbitals and from the  $(2s_a)_2$  orbital. As pointed out in the previous discussion of this molecule, the latter acquires bonding character by being distorted (by charge extraction from Ne) in the



bond directions. The  $sp^3$  hybridized notation is a shorthand way of saying this. When, however, changes in energy are involved, even, for example, in a mechanical model with certain normal vibrations being excited by a periodic force, this force must be resolved with respect to the axis of symmetry of the system and will only feed energy into a normal vibration of its own frequency. In exactly the same way, the interaction of the electric vector of the light wave with the electrons in a molecule must be with those symmetry orbitals which are the irreducible representations of the states involved in the transition moment and the transitions can only occur between states represented by these orbitals. Because of the indistinguishability of electrons, a particular electronic state of an atom or a molecule can only be described in terms of the total probability distribution of negative charge surrounding the positive framework. The orbital structure is manufactured as a consequence of sampling this with dipole radiation. A somewhat similar analogy to the representation of the total wavefunction in terms of orbitals is the representation of a complex wave by its Fourier components, e.g. the sine components of a saw-tooth wave. Orbitals are convenient mathematical functions which are used in combination to represent the total statistical distribution of negative charge in a molecule and are given seeming reality by the nature of the interaction of the molecules with radiation.

### *Spectra and structure of some 'multiple' bonded polyatomic molecules*

In the same way that the spectra and orbital structure of the simple hydrides can be understood by partitioning off protons from the central charge of the inert-gas atoms, the orbital structure of some simple polyatomic molecules can be followed by partitioning off protons from the nuclei of the diatomic molecules with which they are isoelectronic. This is illustrated in Fig. 11. Starting with the well-understood spectrum of  $N_2$ , we pass to HCN by displacing a unit positive charge from one of the nitrogen nuclei to a point further along the bond axis. The movement of the orbitals is indicated by the broken lines. It can be seen that the  $\sigma_{2p}$ , the  $\pi_{2p}$  and the  $\sigma_{2s}$  orbitals have their ionization energies reduced by this

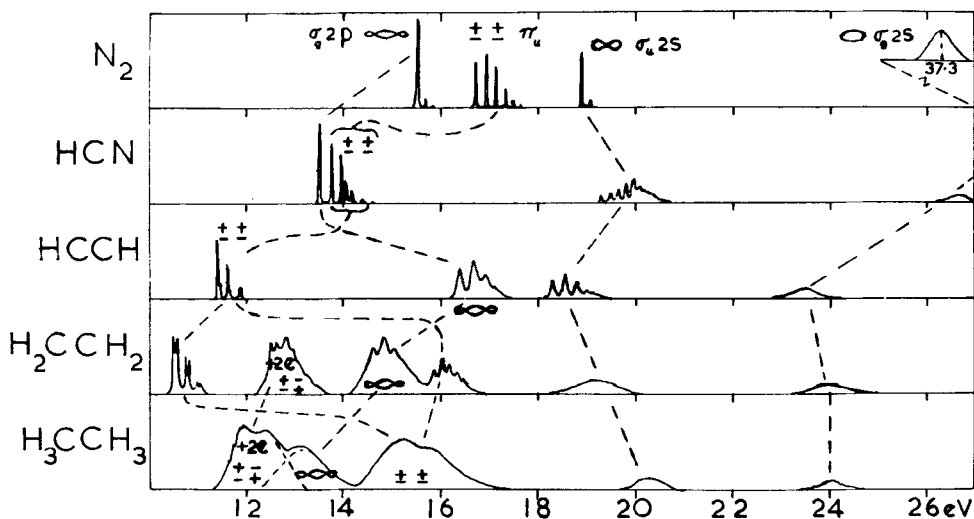


FIG. 11. Photoelectron spectra showing the derivation of the orbitals of HCN and  $C_2H_2$  from the isoelectronic molecule  $N_2$  also related orbitals in  $C_2H_4$  and  $C_2H_6$ .

lessening of the positive charge in the region in which they are mainly located. Another important effect which is apparent from comparison of the spectra is that the  $\pi_u 2p$  electrons lose a considerable amount of their bonding as the nuclei move further away from the position of optimum  $p\pi$  orbital overlap. This can be seen from the change in the intensity distribution of the vibration band pattern (i.e.  $I_{\max}$  moves toward  $I_{\text{adiabatic}}$ ). It is also apparent from the relatively large decrease in ionization energy of this bond orbital. The change from  $N_2$  to HCN affects the  $\sigma_u 2s$  orbital, which now has one of its lobes in the region between the H and the C positive centres. It consequently changes from an antibonding NN to a strongly bonding CH orbital. Its ionization energy is therefore increased and the vibrational pattern of the band changes to one which contains many vibrations of the CH bond reduced in frequency to  $1690\text{ cm}^{-1}$  from the neutral molecular ground-state frequency ( $3311\text{ cm}^{-1}$ ).

A similar partitioning off of charge from the second nitrogen atom leads to the molecule acetylene, in which there is a further increase in central bond distance. The  $\pi_u 2p$ -orbital energy is again lowered by the positive charge reduction and also by loss of bonding due to further removal from its optimum bonding overlap position. The latter effect can be seen in the progressive lowering of the relative intensities of the vibration bands to the first (zero) band of the system. The  $\sigma_g 2s$  and  $\sigma_u 2s$  are reduced in ionization energy by the charge removal, and the latter shows by its vibrational pattern that it is strongly CH bonding, while the former is probably C bonding, though because of its diffuseness, evidence from the vibrational pattern in support of this is not forthcoming. The greatest change in orbital character occurs in the  $\sigma_g 2p$  orbital which becomes strongly CC bonding as the internuclear separation increases toward the optimum value for  $\sigma$ -type bonding. This is indicated by the characteristic bonding envelope of the band pattern in which the CC frequency, reduced to about  $1400\text{ cm}^{-1}$  from its ground-state value of  $1983\text{ cm}^{-1}$ , is strongly excited. It also now exerts some CH bonding, and both combine to raise the ionization energy by nearly 3 eV.

By bringing up two hydrogen atoms on to acetylene and suitably distorting the molecular framework, one can form ethylene. The spectra shows that one of the  $\pi_u$  CC orbitals now becomes the strongly bonding in-phase  $b_{2u}$  ( $\text{CH}_2$ ) orbital, increasing its binding energy by about 4 eV, and the two additional electrons go into the corresponding out-of-phase  $b_{1g}$  ( $\text{CH}_2$ ) orbital. Bringing up two more hydrogen atoms causes the remaining  $\pi$ -electron pair to go into the degenerate in-phase  $e_{1u}$  ( $\text{CH}_3$ ) orbital and the two additional

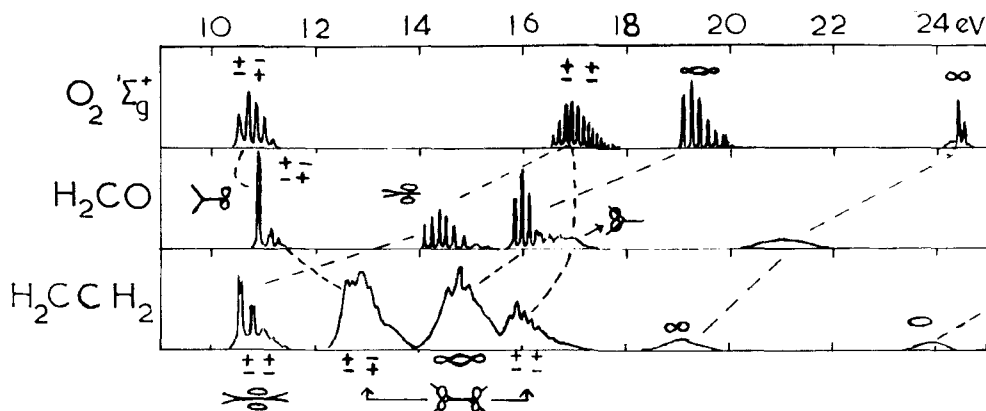


FIG. 12. Photoelectron spectra showing relation of orbitals of  $\text{H}_2\text{CO}$  and  $\text{C}_2\text{H}_4$  relative to those of  $\text{O}_2$ ,  $b^1\Sigma_g^+$ .

electrons to enter the corresponding out-of-phase orbital. In order to cover the complete energy range, these spectra have been taken from recordings with 30.4 nm (40.1 eV) radiation. It can be seen that the separations of the bands corresponding to in-phase and out-of-phase C(2s) combinations (i.e.  $\sigma_g 2s$  and  $\sigma_u 2s$ , respectively) diminishes with increasing CC distances in the molecules  $C_2H_2$ ,  $C_2H_4$  and  $C_2H_6$ . This is a direct result of the reduction in C(2s) orbital overlap as their separation increases.

A similar diagram (Fig. 12) shows how the orbitals of formaldehyde and ethylene are derivable from those of oxygen. Of course in this case it is necessary to start with oxygen in its  $^1\Sigma_g^+$  state, and although the relevant photoelectron spectrum has not been obtained, it can be constructed with confidence from the known spectroscopic data of the state and the photoelectron spectra of  $^3\Sigma_g^-$  and  $^1\Delta_g$ . The spectra show how the antibonding  $\pi 2p$  orbital of oxygen becomes the carbonyl 'lone pair', the  $\pi^4$  orbital splits into the carbonyl  $\pi$  and the  $b_2(CH_2)$ , and the  $\sigma 2p$  becomes the  $a_1(CO)$  bond orbital. Their consistent correlation with the orbitals of ethylene-gives confidence to the general assignment of the orbitals.

### *Spectra and structure of triatomic molecules*

Whether a triatomic molecule is linear or bent in its ground state depends on which configuration best affords coverage of the positive charge by the electrons in the orbitals associated with a particular geometry. Following earlier work by Mulliken, the various ways in which the energies of different orbitals are affected by changing the angle from  $180^\circ$  to  $90^\circ$  were discussed by Walsh (1953) before the advent of photoelectron spectroscopy and are qualitatively described in Walsh diagrams. It is found that molecules with 16 electrons in the valence shell are linear in their ground states (e.g.  $CO_2$ ,  $N_2O$ , etc.). When the number is greater than 16 (e.g.  $NO_2$ ,  $O_3$ , etc.), the molecule has a bent ground state as in  $OF_2$  (20 valence electrons), and this situation persists until the valence shell is completely filled. The structure becomes linear again for  $XeF_2$  (22 outer electrons). For molecules formed from first-row elements, the orbitals can be regarded as being derived from the in-phase and out-of-phase combinations of the 2p orbitals of the outer atoms and the 2p and 2s orbitals of the central atom. The molecular orbitals so constructed for a bent molecule are shown diagrammatically in Fig. 13. For a linear molecule these are very similar and can be visualized by changing the angle to  $180^\circ$ .

In carbon dioxide the orbital of lowest ionization energy corresponds to the out-of-phase combination of 2p(O) orbitals which can be written as  $(\pi_o - \pi_o, \pi_g^4)$ . This splits on bending into  $3b_2$  (in-plane) and  $1a_2$  (out-of-plane) orbitals. As can be seen from the photoelectron spectra shown diagrammatically in Fig. 14, this orbital is nonbonding in the linear triatomic molecules. The next filled orbital is the in-phase  $(\pi_o + \pi_c + \pi_o, \pi_g^4)$  combination which, as expected and indicated by the structure of its band system, is strongly bonding. It splits into  $3a_1$  (in-plane) and  $1b_1$  (out-of-plane) orbitals in the bent molecule. The next inner orbital is that corresponding to the out-of-phase  $(\sigma_o + p\sigma_c - \sigma_o, \sigma_u^2)$  orbital. It is nonbonding and followed by the in-phase  $(\sigma_o + s\sigma_c + \sigma_o, \sigma_g^2)$  bonding orbital. The similar orbital structure in the isoelectronic molecule  $N_2O$  is reflected in its similar photoelectron spectrum. The  $\pi_g$  and  $\sigma_u$  orbitals of this molecule are lower than in  $CO_2$  because they are located near N and O, rather than O and O, atoms. Similarly the  $\pi_u$  and  $\sigma_g$  orbitals are higher in  $N_2O$  than in  $CO_2$  because of the higher energy contribution of the orbitals from the central atoms—N and C, respectively.

In  $NO_2$  the additional electron has to go into the hitherto unfilled  $4a_1$  orbital and the molecule is bent ( $\angle NO = 134^\circ$ ), finding better charge coverage in this geometry. The  $(4a_1)^{-1}$  band appearing on the low-energy side of the photoelectron spectrum, shows a wide vibrational pattern involving the bending motion, since, as might be expected, on ionization from this orbital the molecule moves to the linear structure associated with the 16 electrons

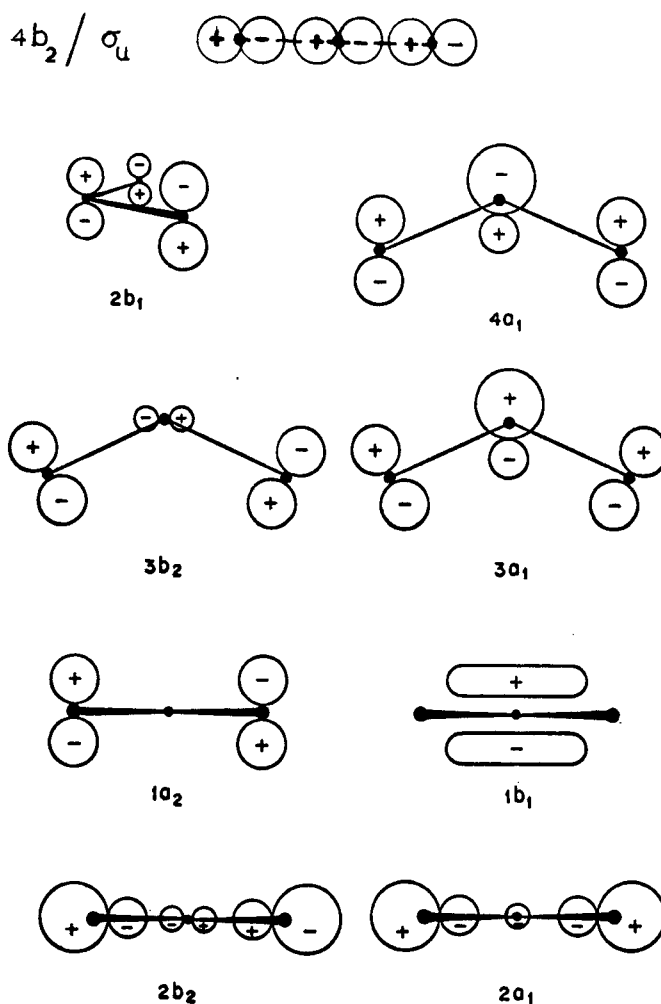


FIG. 13. The valence orbitals of bent triatomic molecules.

then remaining in the valence shell. The orbitals which were doubly degenerate in  $\text{CO}_2$  are split into in-plane and out-of-plane orbitals in bent  $\text{NO}_2$ . Further the states of  $\text{NO}_2^+$  involving ionization from all orbitals apart from the singly occupied  $4a_1$  orbital, are split into singlet and triplet states because of the spin interaction of the two singly occupied orbitals, and they appear in the photoelectron spectrum as pairs of similar systems with a 1 : 3 intensity ratio (Brundle *et al.*, 1970).

The  $4a_1$  shell is filled in  $\text{O}_3$ ,  $\text{SO}_2$  and  $\text{CF}_2$  so that in  $\text{NF}_2$  the additional electron present in its structure has to go into the  $3b_1$  orbital and a new band appears in its photoelectron spectrum. This orbital becomes filled in  $\text{OF}_2$ . The spectrum of  $\text{XeF}_2$ , in which another orbital has to be provided for the two additional electrons, is shown as the final spectrum in Fig. 14. The additional band corresponding to these electrons is evident in the spectrum. Electrons in this orbital are clearly responsible for causing a return to linearity. A full discussion of this spectrum is not possible here.

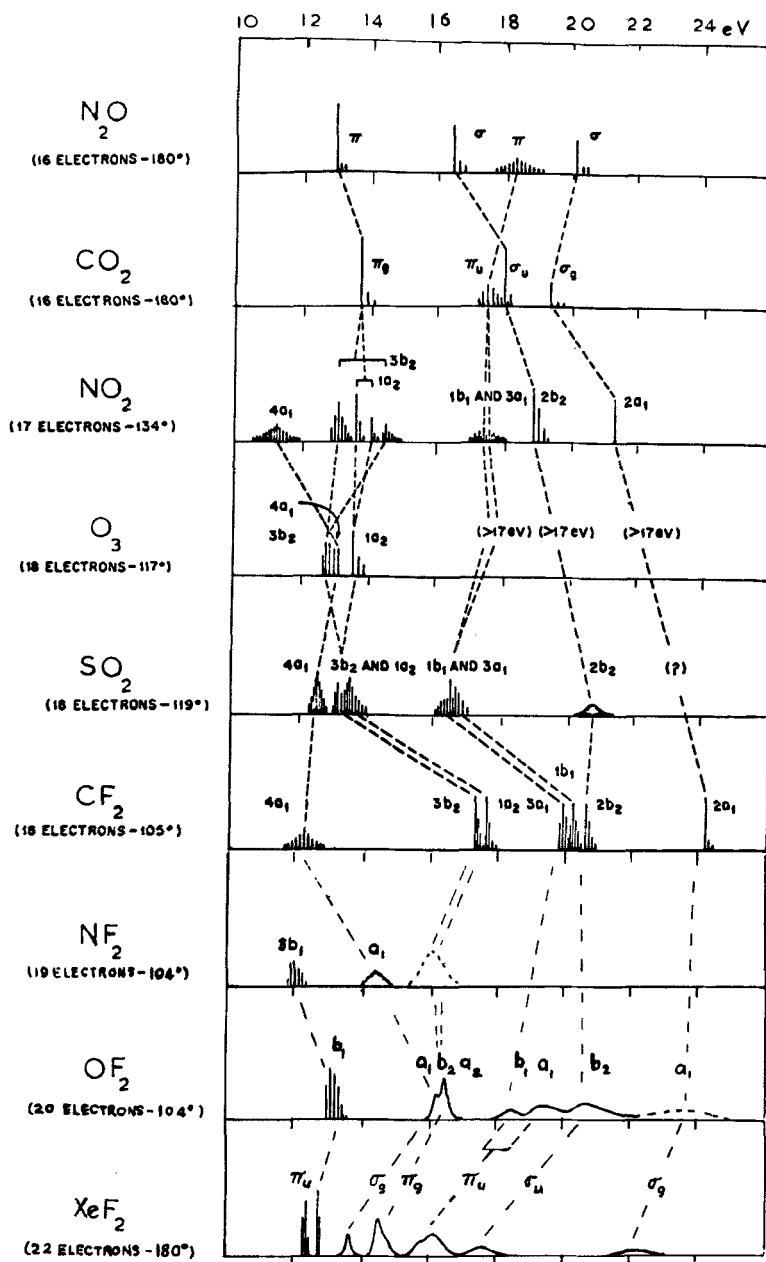


FIG. 14. Diagrammatic photoelectron spectra showing the filling of the orbitals of some triatomic molecules.

The building-up principle illustrated so far for di- and triatomic molecules has been extended to molecules containing four, five, six and seven atoms, particularly for molecules of the type  $AX_n$ , where X is a halogen atom (Potts *et al.*, 1969/70).

While other techniques have to be adopted for more complicated systems, it is clear that a sound understanding of what happens in the simplest cases is a very desirable preliminary to considerations of the larger molecules.

It would be misleading to infer from the foregoing sections that the methods described therein are generally applicable for the analysis of the spectra of more complicated molecules. This is certainly not the case. It is desirable whenever possible to assign bands from direct experimental data, as is the practice in the spectroscopy of simple molecules. However, because the resolution of photoelectron spectroscopy is not adequate to give rotational fine structural details of bands, even if these were present (which they usually are not because of the short lifetimes of the electronic excited states of polyatomic molecules), alternative methods must be used to find the nature of the state to be associated with a band in the photoelectron spectrum.

Obviously the vibrational pattern of a band gives a great deal of information about the orbital from which the electron has been removed, and this is greatly assisted if various isotopic species can be studied. The study of groups of compounds in which one atom is successfully changed to a heavier atom in the same group of the periodic table is also valuable. Any related set of molecules, such as homologous series in which the orbitals of a chromophoric group are modified in a minor way by a substituent, can obviously help assignment. The variation in the relative intensity of the bands with photon energy, the angular dependence of photoelectron cross-sections, and the possibilities of autoionization, are all properties related to the orbital wavefunction, and, if given the proper interpretation, can facilitate assignment. An extension of the 'aufbau' process to build the orbital structures of molecules with more atoms from molecules with fewer atoms (and electrons), is also valuable. Theoretical computations of orbital order, using both *ab initio* and semiempirical approaches, have been widely used to assign the bands of a photoelectron spectrum, and with improvement of molecular parameters, this method has had increasing success.

### *Spectra of ionic molecules*

The binding in the molecules we have so far considered is of the covalent type. In such binding the valence electrons are approximately equally attracted to either of the fragments into which the united atom has been partitioned. When this is not so, as, for example, in the case of LiF, for which the united atom is magnesium (configuration  $1s^2 2s^2 2p^6 3s^2$ ), partitioning off a 3+ fragment will remove first the weakly bound  $3s^2$  electrons to form the  $1s^2$  shell of  $Li^+$  while the more tightly bound  $2p$  electrons will tend to remain in the  $2p^6$  shell, thus forming an  $F^-$  fragment. The field tending to pull over the third electron is clearly dependent on the difference between the ionization potential of the metal atom  $I(M)$  and the electron affinity of the halogen atom  $E_a(X)$ . Values of these differences for the alkali halides range between 2.33 eV for LiF and 0.28 eV for CsCl, whereas for covalent bonds they are much larger, e.g.  $H_2$  or  $CH_3-Cl$ , where the differences would be about 13 and 6 eV, respectively. The  $I(M) - E_a(X)$  differences affect the bonding through the changes which arise in the short-range repulsive forces associated with the overlap of the closed shells of the ions. A study of the electrons in these closed shells by photoelectron spectroscopy might therefore be expected to give direct information concerning the repulsive factors which largely determine the strength of this type of binding.

Photoelectron spectra of the chlorides, bromides and iodides of Na, K, Rb and Cs recorded in the vapour state by a molecular-beam technique are shown in Figs. 15 and 16

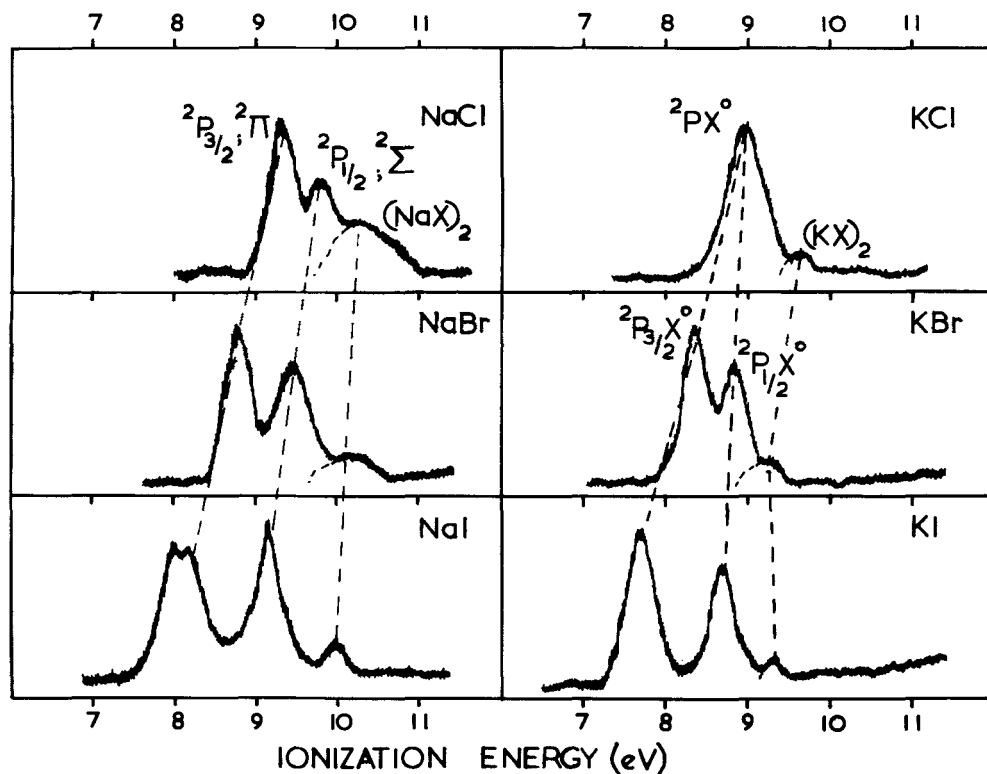


FIG. 15. He I photoelectron spectra of the sodium and potassium halides.

(Potts *et al.*, 1974). All the spectra correspond to the removal of an electron from the  $X^-(p)^6$  shell of the molecule. This produces an  $M^+X^0$  ion in which the ionic bond has been destroyed, leaving only a small residual bonding due to the attraction between the  $M^+$  ion and the induced dipole in the  $X^0$  atom. The photoelectron spectra of the  $M^+X^-$  molecules correspond to transitions to the various states of the  $M^+X^0$  ions, the relative separations of which may be deduced by consideration of the polarization of the  $X^0$  atom by the  $M^+$  ion, i.e. by Stark splitting of the  $^2P$  state of the  $X^0$  atom in fields of different strength for each particular halide. On the basis of Mulliken's treatment (Mulliken 1930), we can represent the probable splitting of the  $X^0$   $^2P$  state by the energy-level diagram shown in Fig. 17. The states of the  $X^0$   $^2P$  atom and their relative energies should correspond to those observed for the  $M^+X^0$  ion in the photoelectron spectra of  $M^+X^-$ . Describing the states of  $M^+X^0$  in terms of the states of the  $X^0$  atom, for the 'zero field' situation, the spectra should show structure corresponding to  $^2P_{3/2}$  and  $^2P_{1/2}$  atomic  $X^0$  states, the separation of the bands being just  $\frac{2}{3}$  times the spin-orbit coupling constant  $\zeta$  for the  $p^5$ ,  $^2P$  state of the free halogen atom. The spectra obtained for the Cs and Rb halides do in fact correspond to just this situation, as might be expected from their low values of  $I(M) - E_a(X)$ , which are 0.280 and 0.563 eV for CsCl and RbCl, respectively, i.e. if any negative charge is placed between  $M^+$  and  $X^0$ , the attraction towards  $M^+$  is largely counterbalanced by that due to the electron affinity of  $X^0$ . The separation found for the  $^2P_{3/2}$  and  $^2P_{1/2}$  bands is as predicted, although in the case of the chlorides the two bands expected are not resolved. For the potassium halides (Fig. 15) the spectra are beginning to show evidence of a polarizing field and show

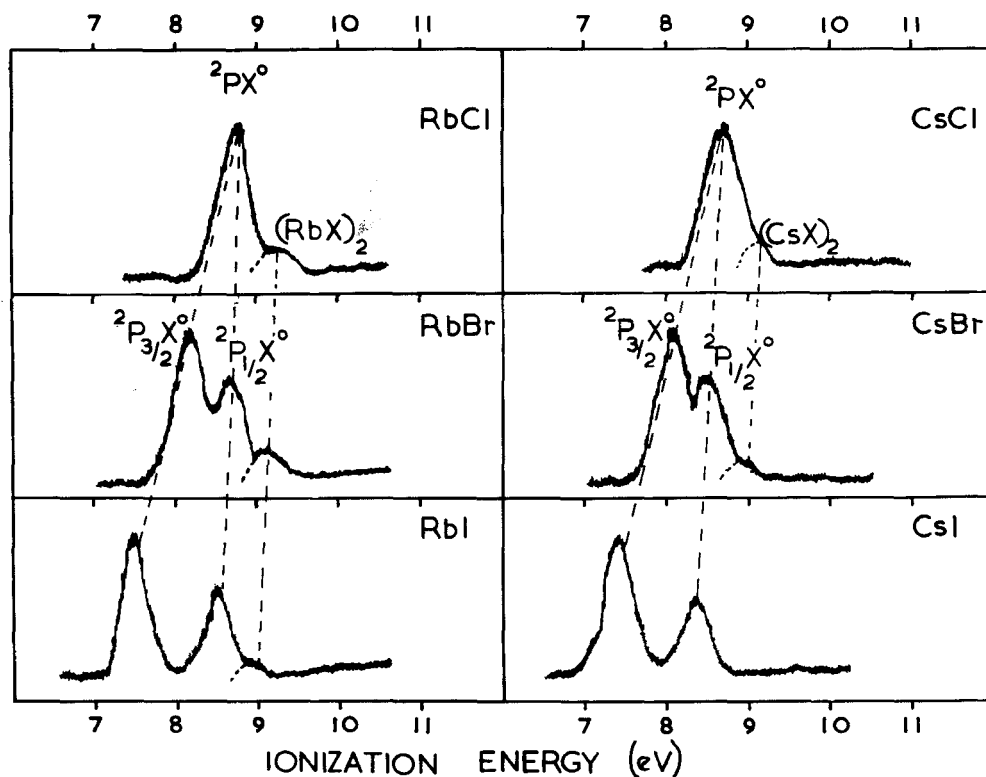


FIG. 16. He I photoelectron spectra of the rubidium and caesium halides.

greater splittings than are found for free X atoms. The spectra of the sodium halides provide examples of polarization ranging from the weak-field to the strong-field situation. For NaI, the  ${}^2P_{3/2}$  state is split into  $M_j = \frac{3}{2}$  and  $\frac{1}{2}$  components and the  ${}^2P_{3/2} - {}^2P_{1/2}$  splitting is slightly greater than  $\frac{3}{2}\zeta$ . In the spectrum of NaBr, the  ${}^2P_{3/2} - {}^2P_{1/2}$  splitting is increased to 0.65 eV as compared with a value of 0.46 eV expected for zero electric field, while for NaCl the splitting is increased from 0.11 eV to 0.46 eV. These indications of the presence of large fields agree with the relatively large  $I(M) - E_a(X)$  differences, which are 1.525, 1.775 and 2.075 eV for NaCl, NaBr and NaI, respectively.

Features to the high-ionization-energy side of the  $(p)^{-1}$  bands observed in a number of the spectra are attributed to ionization of the  $(MX)_2$  dimer, which will be present in increasing amounts for the lighter halides. Comparison with the reliable values for the polymer (solid crystal), which are now available (Poole, 1973), shows that the energies required to ionize the dimers and polymers are greater than those needed for the monomer. The greatest increment occurs in going from monomer to dimer, the subsequent changes being an order of magnitude smaller. For example, the first ionization potential of NaCl is 9.34 eV, that of  $(NaCl)_2$  is 0.96 eV higher, while that of  $(NaCl)_n$  crystal is raised still further by 0.15 eV. These increments are clearly due to increases in the polarization stabilization of the ionized states of  $Cl^-$  arising from the increasing population of its environment by polarizable ions. At present we are still at an early stage in the study of ionic binding by photoelectron spectroscopy, but valuable new information has been accumulated (Berkowitz *et al.*, 1973).



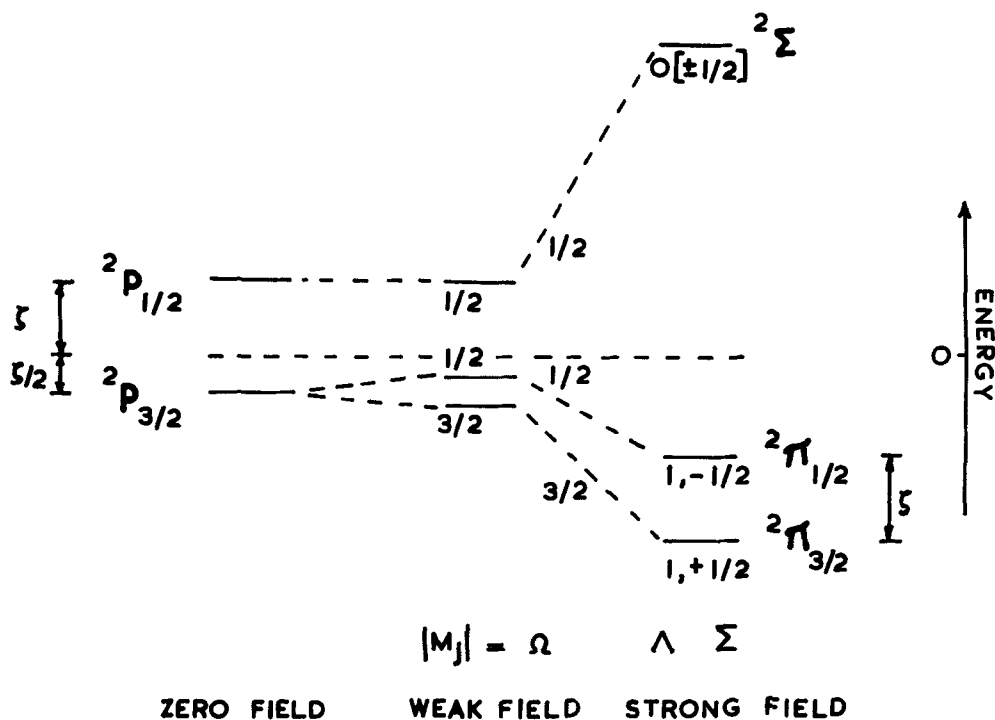


FIG. 17. Correlation of the various energies of ionized states formed by Stark splitting of the  $X^0 2P$  state.

#### *Spectra of some simple aromatic molecules*

Although this review is primarily concerned with relatively small molecules, it could hardly omit a brief account of the photoelectron spectrum of benzene and some of its simple derivatives, because of the great importance of the electronic arrangement in the aromatic nucleus which is responsible for the special properties of six-membered  $\pi$  ring systems. Such systems are too large to be treated by the united-atom techniques, and orbital assignments must be made by comparison of the bands observed in the photoelectron spectrum with the set of molecular orbitals which can be formed by combining atomic orbitals into orthogonal sets appropriate to the molecular geometry. Jonsson and Lindholm (1969) made the first assignment of the benzene spectrum based on several different types of information, including SCF calculations. More recently further information has been obtained on the nature of the bands from measurements of the relative band intensities in spectra obtained with Ne I, He I, He II, and Mg K( $\alpha$ ) irradiation, from detailed analyses of the few bands which have resolvable vibrational fine structure, from angular distributions of the photoelectrons, from comparisons with Rydberg series, and from photoionization cross-section mass spectrometric studies. After a certain amount of controversial discussion, the Jonsson and Lindholm orbital assignment is now firmly established. It is shown in Fig. 18. Using this assignment, the orbital structure of benzene omitting C(1s) combinations can be written in a simplified form as  $s^2s^4s^{*4}r^2s^{*2}t^4\pi^2t^4\pi^4$  where  $s$  corresponds to orbitals built from C(2s) orbitals,  $t$  to orbitals built from C(2p) orbitals orientated tangentially to the ring,  $r$  orbitals constructed from C(2p) + H(1s) orbitals orientated radially, and  $\pi$  orbitals from C(2p) orbitals orientated perpendicular to the

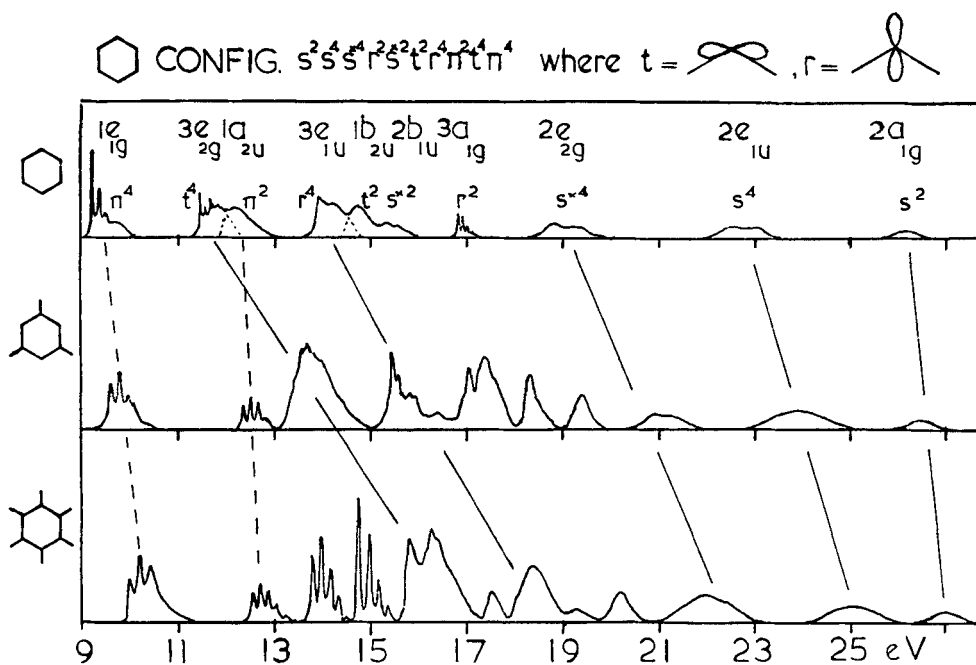


FIG. 18. Photoelectron spectra of benzene, 1,3,5-trifluorobenzene and hexafluorobenzene (composite He I and He II spectra).

molecular plane. The successive orbitals are simply the various linear combinations of the atomic orbitals which have progressively increasing numbers of nodal surfaces. The order in which they are given is that of binding energy decreasing from left to right. Writing these orbitals in terms appropriate to  $D_{6h}$  symmetry, the ground-state configuration of benzene is  $(2a_{1g})^2(2e_{1u})^4(2e_{2g})^4(3a_{1g})^2(2b_{1u})^2(3e_{1u})^4(1a_{2u})^2(3e_{2g})^4(1e_{1g})^4$ . Molecular orbital calculations can be used to identify some of the bands directly. All calculations indicate that the first ionization potential at 9.25 eV is to be identified with  $(\pi, 1e_{1g})^{-1}$  ionization. This is supported by the appearance in its vibrational pattern of vibrations of  $e_{2g}$  symmetry, in addition to totally symmetrical vibrations. Jahn-Teller splitting would normally be expected on ionization of the  $(1e_{1g})^4$  filled shell, but the bonding power of the electrons is so small in this case that the only indication of the degeneracy of the ionic state is the appearance of the  $e_{2g}$  vibrations in single quanta (Potts *et al.*, 1973).

The next  $\pi^{-1}$  ionization potential  $(1a_{2u})^{-1}$  is expected to lie in the 12 eV region but as this is also where the ionization  $(t, 3e_{2g})^{-1}$  is expected to occur some uncertainty has existed in the assignment in this region. Various features of the photoelectron spectrum in the region 11.4–13.4 eV have been invoked to try to settle this question but as only a small part of it shows sharp structure, a satisfactory understanding of this region has taken some time to achieve. A deeper understanding of the vibrational pattern in terms of the Jahn-Teller effect as well as shifts and splittings brought about by various F substitutions (*see later*) now appear definitely to favour the assignment shown in Fig. 18, as originally suggested by Jonsson and Lindholm. All the other assignments of bands in the photoelectron spectrum to orbitals of the valence electrons are now generally accepted and since for hydrocarbons the bottom of the valence shell can be reached with He II radiation, our knowledge of the valence-shell orbitals of benzene is complete. Photoelectron spectroscopy has certainly

revealed the orbital structure of this 12-atom molecule to a degree which a decade ago seemed beyond our reach.

### The spectra of some fluorobenzenes

Some interesting points on the effect of substituents on group orbital systems are illustrated in the spectra of the fluorine-substituted benzenes shown in Figs. 18 and 19. These have relevance to the orbital assignment of the bands in benzene itself. Figure 18 compares the spectrum of 1,3,5-trifluoro- and hexafluoro-benzene with that of benzene. The mixing of  $2p\pi$  F orbitals into the  $\pi^4$  and  $\pi^2$  orbitals is well known to cause little shift of  $\pi$  levels, due to the compensation of the blue-shifting inductive effect by an opposing mesomeric effect involving repulsion between filled orbitals of the same symmetry (Bralsford *et al.*, 1960). The in-plane  $t$  orbitals in 1,3,5-trifluoro- and hexafluoro-benzene, on the other hand, suffer large shifts to higher energies because of the predominance of the inductive over the mesomeric effect for in-plane orbitals. This separates the  $1a_{2u}$  clearly from the  $3e_{2g}$  orbitals and the spectra of the tri- and hexa-fluorobenzenes show the  $1e_{1g}$  and  $1a_{2u}$  bands appearing in clearly recognizable form with an expected intensity ratio of 2/1.

Figure 19 shows the substitutional splitting of the  $(1e_{1g})^4$  orbital as we pass to  $C_{2v}$  symmetry in going from benzene to monofluorobenzene and to *p*-difluorobenzene. The doubly degenerate orbitals  $(1e_{1g})^4$  now split into two mutually orthogonal components. One of these is a  $2b_1$  orbital, which has a nodal surface perpendicular to the molecular

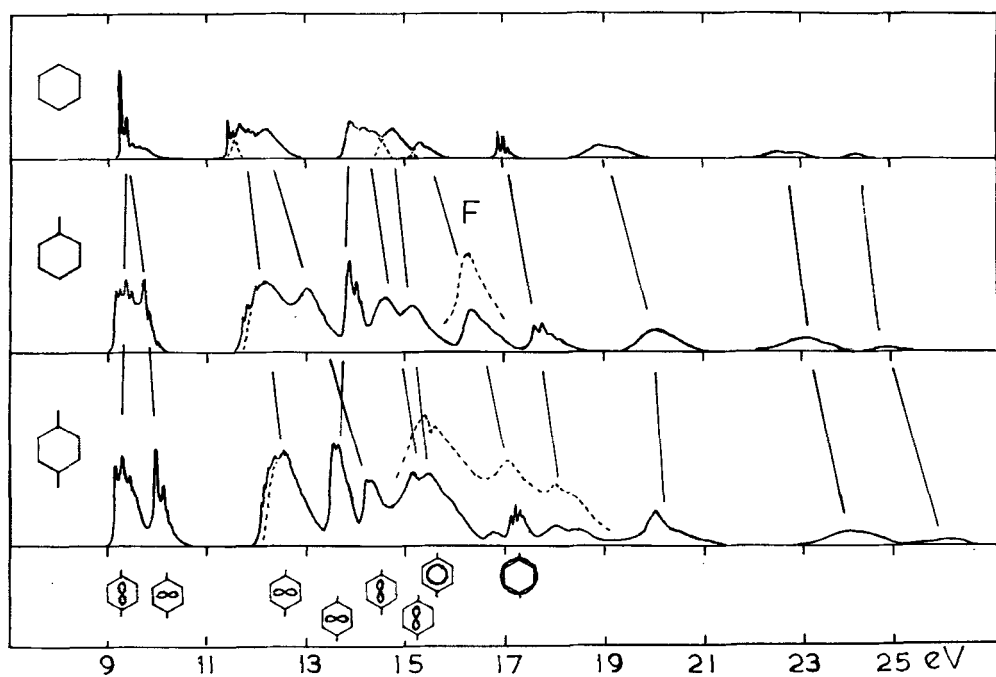


FIG. 19. Photoelectron spectra of benzene, monofluorobenzene and *p*-difluorobenzene.

Total bond energies of negative, neutral and positive species of first row hydrides  
 $(X^{-,0,+}H_n \rightarrow X^{-,0,+} + nH)$

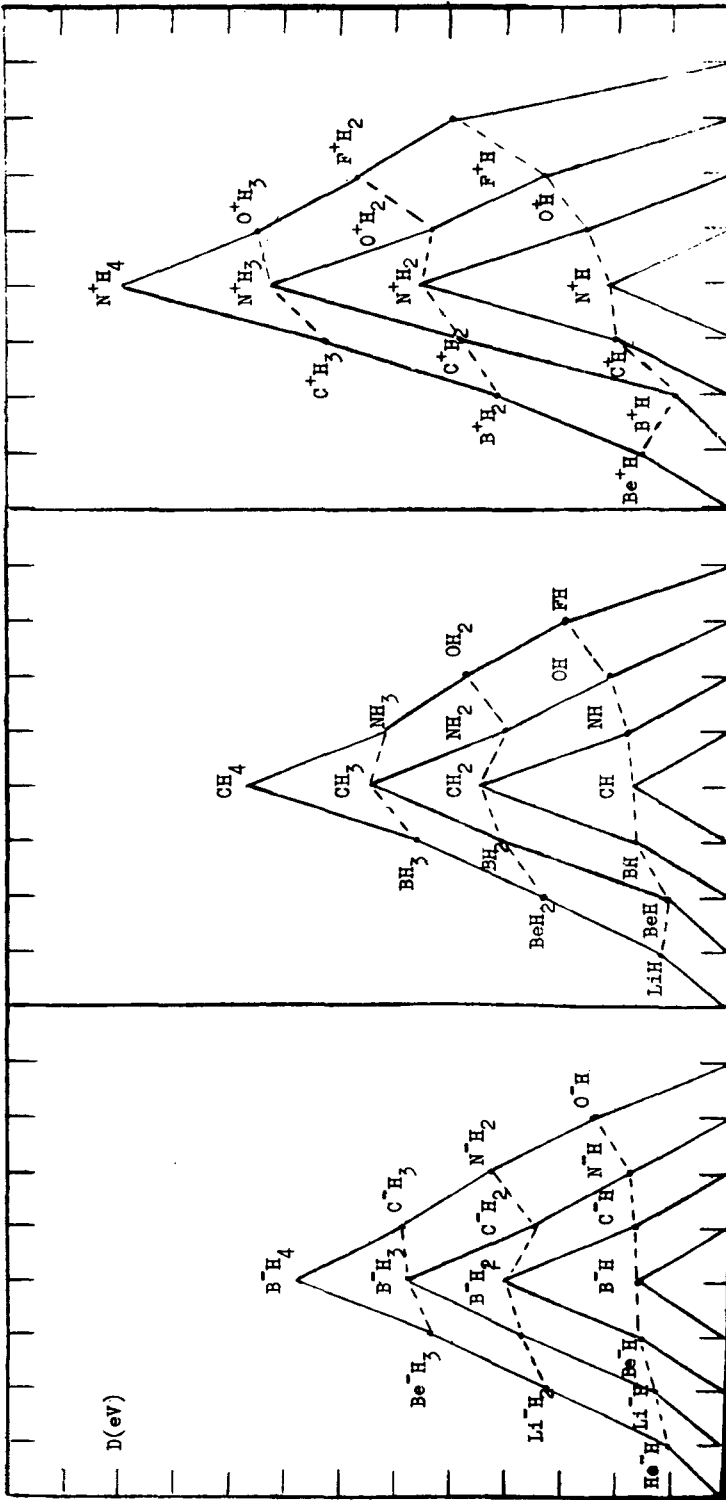


FIG. 20. Energies of atomization of the negative, neutral and positive species of the first row hydrides.

plane and passing through the CF bond. This orbital is therefore unaffected by the substitution. The other is a  $1a_2$  orbital, one lobe of which overlaps the  $2p\pi$  F orbital and therefore interacts with it (see Lindholm, 1973). These orbital differences are strikingly confirmed by the vibrational patterns observed in the two photoelectron bands into which the first benzene band divides. The first of these shows a fairly wide vibrational pattern and indicates that it corresponds to ionization from the  $1a_2$  orbital which overlaps the  $2p\pi$  F orbital. The vibrational pattern of the second band is hardly altered from that of unsubstituted benzene and is thus to be correlated with the  $2b_1$  orbital, which has a nodal plane passing through the CF bond. The vibrational pattern of the first band is not in fact greatly different from that of the  $1a_{2u}$  orbital ( $1b_1$  in  $C_{2v}$  symmetry) which must also overlap the  $2p\pi$  F orbital. Although this cannot be seen in the spectra of Fig. 19, it becomes clear in the spectra of the tetrafluorobenzenes, where the  $(1a_{2u})^{-1}$  band is well separated from the band systems arising from in-plane orbitals.

The orbital interactions arising from the insertion of  $(2p\pi_{x,y})^4$  electrons with every F substitution differ somewhat for the in-plane orbitals from those for the  $\pi$  orbitals just discussed. These differences afford valuable criteria for orbital identification. A  $2p$  F orbital lying in the molecular plane and perpendicular to a CF bond can interact mesomerically with a  $\sigma$  ring orbital which happens to have a major nodal plane coinciding with the nodal plane of the  $2p$  F orbital. A band associated with such an orbital would not be shifted so much to high energies as one associated with another (orthogonal) orbital for which the inductive effect of the fluorine was not compensated by opposing mesomeric repulsion. In the  $C_{2v}$  symmetry situation arising in mono and *p*-difluoro-benzene, it is clear from Fig. 19 that the band system assigned as due to  $3e_{2g}^{-1}$  ionization is split by the substitution, the lower ionization potential half suffering minor, and the higher ionization potential half suffering major, shifts to higher energies. Reference to the orbital diagrams shows that such behaviour is to be expected if these orbitals are respectively  $7b_2$  and  $11a_1$  species in  $C_{2v}$  symmetry. The shape of the singly degenerate  $t^2$  orbital  $1b_{2u}$  indicates an appreciable mesomeric effect and thus a small shift is to be expected for this band. In 1,3,5-trifluoro and hexafluorobenzene, where  $D_{3h}$  and  $D_{6h}$  symmetries pertain, there can be no mesomeric effect for the in-plane orbitals as in  $C_{2v}$  symmetries. Consequently there is no substitutional splitting of band systems, and all orbitals are shifted to higher energies by unopposed inductive effects. These features are indicated by connecting lines in the figures. Similar behaviour is shown by the in-plane  $r^4$  and  $r^2$  systems, as shown by the  $t^4$  and  $t^2$  systems with respect to changes in molecular symmetry arising from F substitution. The two sharp band systems in hexafluorobenzene appearing in the range 13.5–15.5 eV seem to be the  $\pi^{*2}$ ,  $\pi^{*4}$  which, together with the  $\pi^4$  and  $\pi^2$  set at higher energies, account for the twelve  $2p\pi$  F electrons of the  $C_6F_6$  molecule.

#### *Photoelectron spectra of large polyatomic systems—large organic molecules, solids, etc.*

Since a photoelectron band is to be expected for every occupied electron orbital, the number of bands in a spectrum is very large for large molecules and they overlap and merge into one another as the molecular size increases. The spectrum is then best described in terms of a diagram of density-of-states. In the case of a metal, the outer *s*, *p* or *d* atomic orbitals which overlap combine to form conduction bands with density-of-states contours related to the various atomic orbitals from which they are derived. In the case of large organic molecules, the presence of different conformers each with a different spectrum further complicates matters. In spite of these difficulties, much valuable information can be obtained from the spectra of such molecules and their treatment has been discussed by Heilbronner and Maier (1977). The low-energy regions of the spectra generally are associated with conjugated  $\pi$  systems and lone pairs of N, O and S, and from these regions

important information about hydrogen bonding, steric effects, through-bond and through-space interactions, can be derived. Numerous other applications of photoelectron spectroscopy are discussed in two recent books on the subject (Rabalais, 1977; Brundle and Baker, 1977).

## CONCLUSION

Before closing this review, we wish to emphasize that ionization and dissociation energy are closely related, both being part of the electrostatic attraction between the nuclear framework and the total electron cloud (statistically distributed according to quantum requirements). The ionization potential of a molecule is given by  $I_M = I_A + D_M - D_{M^+}$  and as the atomic ionization potential  $I_{2A}$  and the dissociation energy in the ground state  $D_M$  are usually known, then  $D_{M^+}$  can be calculated from a knowledge of  $I_M$ , which can be found by photoelectron spectroscopy if it is not already known. Sets of diagrams similar to those in Fig. 20 can be constructed which correlate the atomization energies of related groups of molecules, and provide a basis for understanding their chemical behaviour in terms of their electrical properties. Thus in the positive-ion world,  $NH_4^+$  and  $OH_2^+$  are stable moieties. In the negative-ion world, for which a knowledge of electron affinities is necessary,  $BH_4^-$ ,  $CH_3^-$ ,  $NH_2^-$  and  $OH^-$  are the species isoelectronic with the stable molecules  $CH_4$ ,  $NH_3$ ,  $H_2O$  and  $HF$ .

Finally attention is called to a paper by Beamson, Porter and Turner (1979) describing an instrument in which photoelectrons ejected from a surface by He I radiation are used in an electron microscope device based on the highly diverging magnetic field of a superconducting magnet to form an image of this surface. Thus the possibility of photoelectron microscopy with point-by-point analysis of surfaces seems to be an intriguing future development of this powerful technique.

We make no apologies for excluding discussion of XPS from this review, since it will no doubt be the subject of a future review. Even the briefest account would have occupied the major part of the space allocated for the present article.

## REFERENCES

- BEAMSON, G., PORTER, H. Q. and TURNER, D. W. (1979). *J. Phys. E*, 313, 64.  
 BERKOWITZ, J., DEHMER, J. L. and WALKER, T. E. H. (1973). *J. Chem. Phys.*, 59, 3645.  
 BRALSFORD, R., HARRIS, P. V. and PRICE, W. C. (1960). *Proc. R. Soc.*, A258, 459.  
 BRUNDLE, C. R. and BAKER, A. D. (1977). *Electron Spectroscopy*, vol. 1, p. 273. London, NY: Academic Press.  
 BRUNDLE, C. R., NEUMAN, D., PRICE, W. C., EVANS, D., POTTS, A. W. and STREETS, D. G. (1970). *J. Chem. Phys.*, 53, 705.  
 FEYNMAN, R. P. (1939). *Phys. Rev.*, 56, 340.  
 JONSSON, B. O. and LINDHOLM, E. (1969). *Ark Fysik*, 39, 65.  
 KOOPMANS, T. (1934). *Physica*, 1, 104.  
 MULLIKEN, R. S. (1930). *Rev. Mod. Phys.*, 2, 60.  
 POOLE, R. T., LIESEGANG, J., LECKEY, R. C. G. and JENKIN, J. G. (1973). *Chem. Phys. Lett.*, 23, 194.  
 POTTS, A. W., LEMPKA, H. J., STREETS, D. G. and PRICE, W. C. (1969/70). *Phil. Trans. R. Soc., Lond.*, A268, 59.  
 POTTS, A. W. and PRICE, W. C. (1972). *Proc. R. Soc., Lond.*, A326, 165, 181.  
 POTTS, A. W., PRICE, W. C., STREETS, D. G. and WILLIAMS, T. A. (1973). *Discuss. Faraday Soc.*, 54, 168.  
 POTTS, A. W., PRICE, W. C. and WILLIAMS, T. A. (1974). *Proc. R. Soc., Lond.*, A341, 147.  
 PRICE, W. C. (1936). *J. Chem. Phys.*, 4, 147 and 539.

- PRICE, W. C. (1977). In *Electron Spectroscopy* (eds. C. R. Brundle and A. D. Baker), vol. 1, p. 152. London, NY: Academic Press.
- RABALAIS, J. W. (1977). *Principles of Ultraviolet Photoelectron Spectroscopy*. NY, London: John Wiley and Sons.
- SIEGBAHN, K., NORDLING, C., FAHLMAN, A., NORGBERG, R., HAMRIN, K., HEDMAN, J., JOHANSSON, G., BERGMARK, T., KARLSON, S. E., LINDGREN, I. and LINDBERG, B. (1967). *ESCA—Atomic, Molecular and Solid State Structure Studies by means of Electron Spectroscopy*. Amsterdam, NY: North Holland Pub. Co.
- SIEGBAHN, K., NORDLING, C., JOHANSSON, G., HEDMAN, J., HEDEN, P. F., HAMRIN, K., GELIUS, V., BERGMARK, T., WERME, L. O., MANNE, R. and BAER, Y. (1967). *ESCA—Applied to Free Molecules*. Amsterdam, NY: North Holland Pub. Co.
- TURNER, D. W. and AL JOBORY, M. I. (1962). *J. Chem. Phys.*, *37*, 3007.
- VILESOV, F. I., KURBATOV, B. C. and TEREININ, A. N. (1961). *Dokl. Akad. Nauk SSSR*, *138*, 1320; (1962) *Soviet Phys. Dokl.*, *8*, 883.
- WALSH, A. D. (1953). *J. Chem. Soc., Lond.*, pp. 2260 and 2266.
- WATANABE, K. and MOTT, J. R. (1957). *J. Chem. Phys.*, *26*, 1773.